Computer Control of an Enthalpy Exchanger

Jensen, Lars; Hänsel, Richard

1974

Document Version:
Publisher's PDF, also known as Version of record

THE LUND INSTITUTE OF TECHNOLOGY

DEPARTMENT OF
BUILDING SIENCE

DIVISION OF
AUTOMATIC CONTROL

REPORT 1974:8

Computer control of an enthalpy exchanger

L H Jensen
R Hänsel

COMPUTER CONTROL OF AN ENTHALPY EXCHANGER

L.H. Jensen
R. Hänsel

This work has been a cooperation between the Department of Building Science and the Division of Automatic Control, Lund Institute of Technology, Lund and the Swedish Steam Users Association, Malmö. The work is also a part of a research project supported by Grant D698 from the Swedish Council for Building Research.

Abstract

An enthalpy exchanger is studied as a temperature exchanger. Static and dynamic models based on construction data are developed. Static and dynamic models are also derived from experimental data. The process is very nonlinear. This is seen in the models. The static gain varies with a factor about 100. The dynamic is rather fast. A controller with fix parameters will have a bad performance. A simple selftuning regulator is implemented and tested in fullscale experiments with good result.

Table of contents

1	Introduction	1
2	Process	3
3	Simple process models	7
3.1	A compartment model	8
3.2	A sector element model	13
4	Process models based on experiments	18
4.1	Measurement and control equipment	18
4.2	Determination of temperature efficiency using experimental data	23
4.3	Dynamic models based on experiments	27
4.4	Startup fenomena	31
5	Determination of a regulator	33
5.1	Background	33
5.2	A selftuning regulator	36
6	Fullscale control experiment	40
6.1	Implementation of a selftuning regulator	40
6.2	A selftuning regulator with one parameter	42
6.3	A selftuning regulator with two parameters	45
7	Conclusions and remarks	50
8	References	52

1 Introduction

This report is the result of a cooperation between the Department of Building Science, the Division of Automatic Control, both Lund Institute of Technology and the Swedish Steam User's Association (Angpanneföreningen), Malmö.

The main purpose with the work is to study how an enthalpy exchanger can be controlled. The controlled variable is the air temperature after the enthalpy exchanger. No attempt is made to control both air temperature and air absolute moisture. The enthalpy exchanger will only be studied as an temperature exchanger throughout the report. The input is the revolution speed of the rotor.

The static relation between the output and the input is nonlinear. The static gain depends also of the two other uncontrollable inputs the outdoor and exhaust air temperature. These effects makes the process rather difficult to control.

Two simple models of the enthalpy exchanger are derived in section 3. These model's are far from perfect but the intention is to give a crude model of the exchanger.

Models have also been identified from data from specially made experiments. The result is given in section 4 together with a short description of the measurement and control equipment.

The process is very nonlinear. A regulator with constant parameters will in general have an unsatisfactory performance. Thus a regulator with adjustable parameters might be a solution. A simple selftuning regulator is developed in section 5.

In section 6 some fullscale control experiments are made with the selftuning regulator with good result.

Finally some conclusions are drawn and some remarks are made about the experiments in section 7.

2 The process

The information about the process has been taken from the manufacturer's catalogue (Munters' Econovent AB).

A good picture of the enthalpy exchanger is given in figure 2.1. In figure 2.2 it is shown where an enthalpy exchanger is situated in a normal climate system.

An enthalpy exchanger can exchange both temperature and absolute moisture between two airstreams. It consists of a rotor of many axial channels. The channel diameter is about 1.5 mm. This gives a large contact surface between the air and the rotor per rotor volume of about 3000 m^2/m^3. The outdoor air passes one half of the rotor and the exhaust air passes the other half of the rotor in the opposite direction. The rotor rotates with 10 revolutions per minute at maximum speed. An axial channel of the rotor will then exchange enthalpy with the outdoor air and with the exhaust air for about 3 seconds each.

Recirculation of exhaust air is prevented by a small purging sector between the exhaust air and outdoor air.

The exchange of temperature and moisture or enthalpy is shown in figure 2.3. The efficiency is given as a function of the revolution speed in figure 2.4. The proportion between different revolution speeds during a whole year can be seen in figure 2.5.

The enthalpy exchanger to be considered in this report is situated in the Swedish Steam Users' Association office building at Malmö. Some data are as follows:

type Munters EV 1900
installed in 1971
outdoor air flow 17750 m^3/h

exhaust air flow 18050 m^3/h
leakage flow over purging sector 600 m^3/h
rotor diameter 1900 mm
rotor thickness 200 mm
maximum revolution speed 8.6 r/min (measured)
motor Groschopp & Wiersen
M 94-60 380 V 0.65 A 3000 r/min
motor drive unit Tyrovent 313-103
card 80-2152B
motor potentiometer SQD2 P10
stroke time 75 sec
stroke angle 90^0
potentiometer 220 Ω
temperature sensor RCA1(X) GT

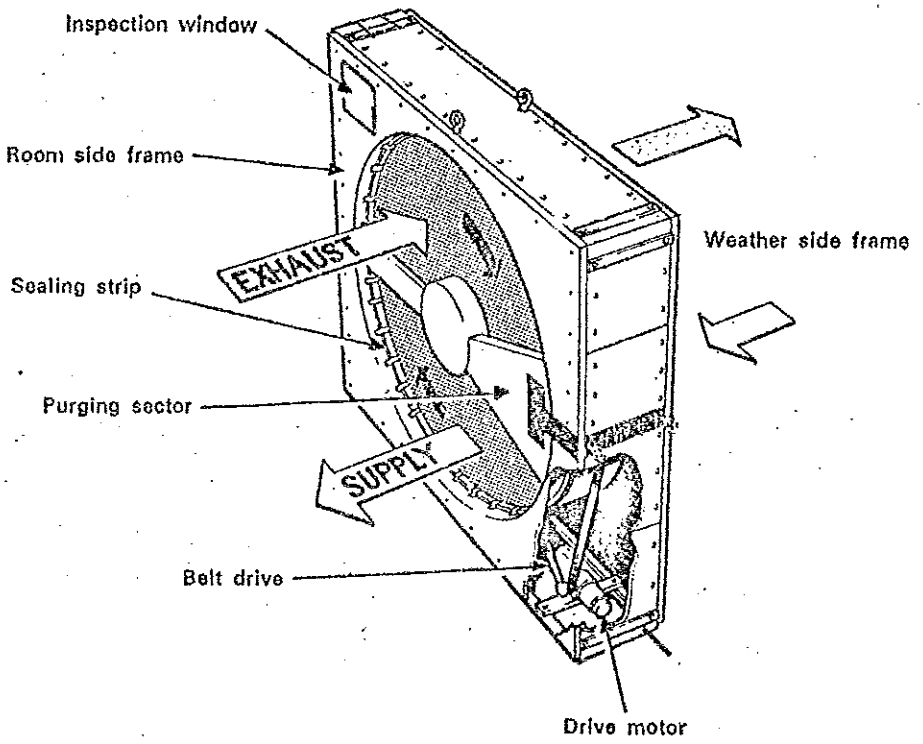

Figure 2.1 The main parts of an enthalpy exchanger

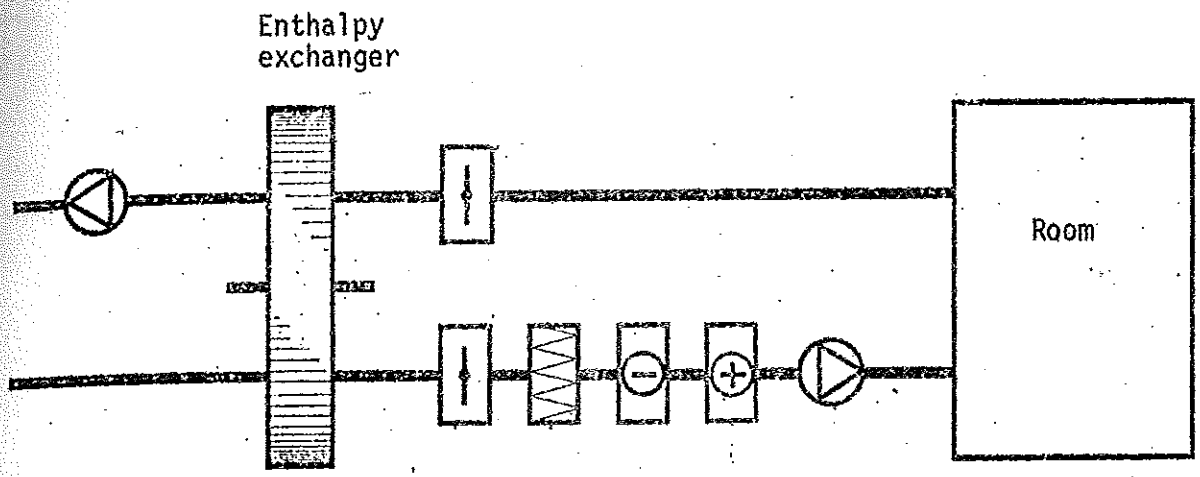

Figure 2.2 A climate system with an enthalpy exchanger

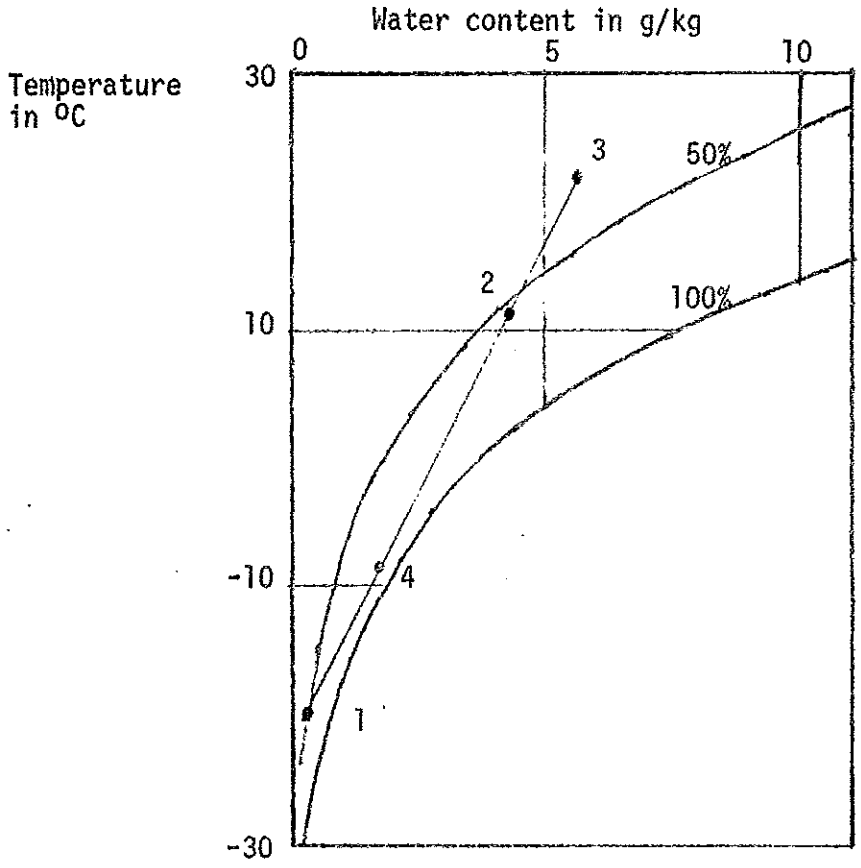

Figure 2.3 An example in a Mollier diagram how an enthalpy exchanger works with 75% efficiency

1 Outdoor air before exchanger
2 Outdoor air after exchanger
3 Exhaust air before exchanger
4 Exhaust air after exchanger

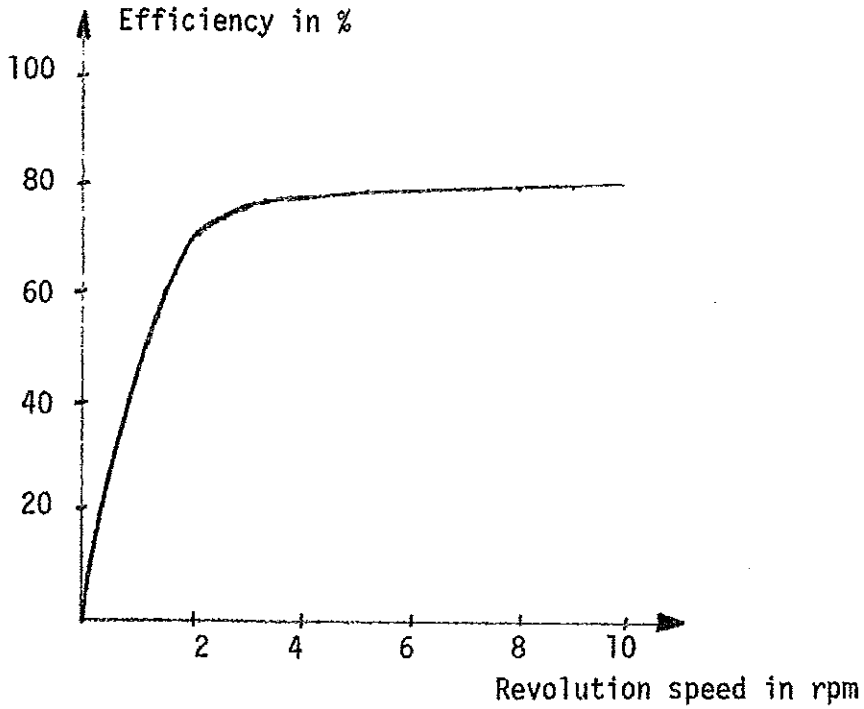

Figure 2.4 Efficiency as a function of revolution speed

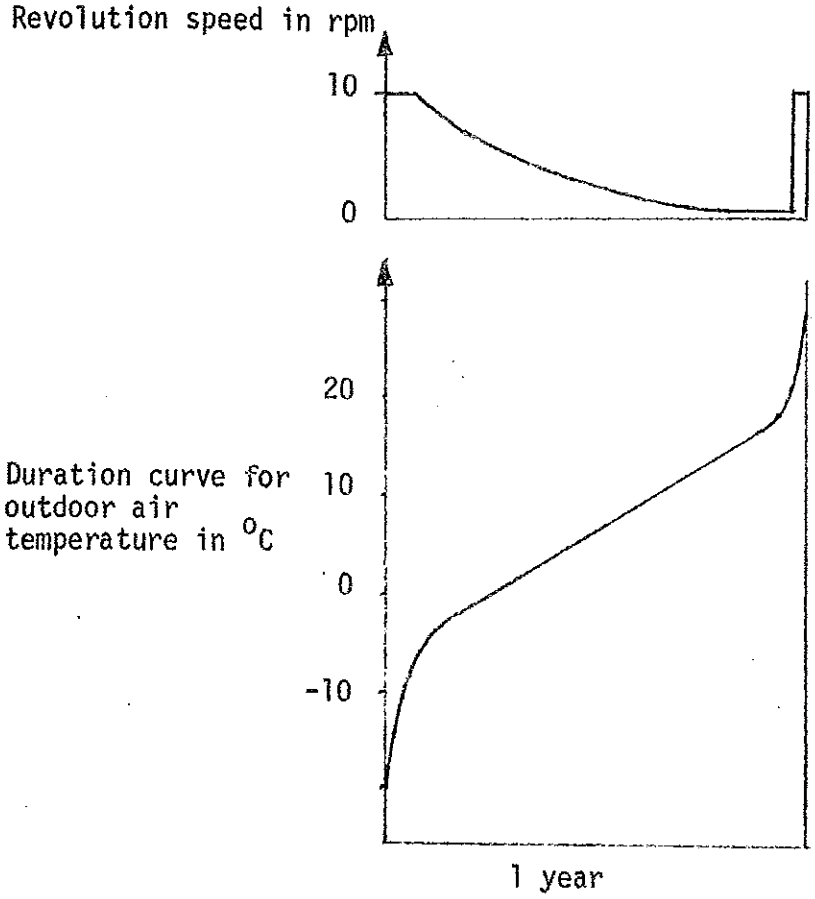

Figure 2.5 The revolution speed as a function of the duration of outdoor air temperature during one year.

3 Simple process models

The purpose with this report is not to develop a complete model for an enthalpy exchanger, but to study simple models with the main properties of an enthalpy exchanger.

In this section the enthalpy exchanger will be regarded as a pure temperature exchanger with no possibility to exchange water.

It is possible to set up two partial differential equations for the enthalpy of the rotormaterial and the air in the rotor. This can be done by studing the temperature balance of a small axial and sector element. The model will be distributed in both axial direction of the rotor and in angular direction, but naturally not in radial direction. It is possible to solve this set of two coupled partial differential equation together with the boundary conditions on a large computer.

A compartment model, which first is lumped in both angular and axial direction, is used in section 3.1 to study both static and dynamic properities. This model is later extended in axial direction. A model, which is lumped only in axial direction, is given in section 3.2. A small angular element of the rotor is studied during one revolution in steady state. The temperature efficiency can then be derived as a function of the revolution speed.

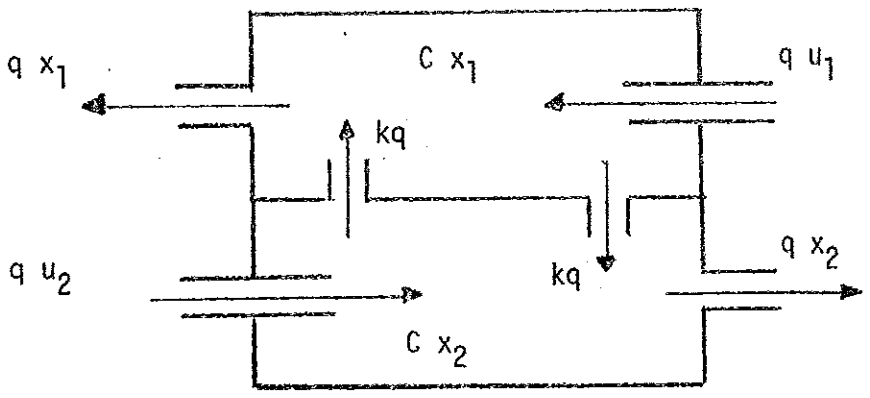

Figure 3.1 A compartment model of a enthalpy exchanger

3.1 A compartment model

The model is shown in figure 3.1. The assumptions that are made in this model are as follows:

1 The air and rotor temperature are the same throughout the whole outdoor air sector

2 The air and rotor temperature are the same throughout the whole exhaust air sector

3 The purging sector is neglected

The inputs of the model are the outdoor air temperature $u_1(t)$ and the exhaust air temperature $u_2(t)$.

The first state $x_1(t)$ is the temperature of the rotor and the air in the outdoor air sector. The second state $x_2(t)$ is the temperature of the rotor and air in the exhaust air sector.

The outputs are the two states of the model.

A flow of magnitude q passes each compartment. A flow of magnitude kq circulates between the two compartments. This second flow is assumed to correspond to the revolution speed.

Two coupled differential equations can be set up for the two states of the model. These are as follows:

$$C\,\dot{x}_1 = q(u_1-x_1) + kq\,(x_2-x_1) \qquad (3.1)$$

$$C\,\dot{x}_2 = q(u_2-x_2) + kq(x_1-x_2) \qquad (3.2)$$

The time unit can be chosen so that C = q. The equations can be simplified to:

$$\dot{x}_1 = -(k+1)x_1 + k\,x_2 + u_1 \qquad (3.3)$$

$$\dot{x}_2 = -(k+1)x_2 + k\,x_1 + u_2 \qquad (3.4)$$

The model is nonlinear if the revolution speed is supposed to be an input to the model.

How is the value of k related to the maximum revolution speed? At maximum speed is the efficiency about 75%. Assume that the exhaust air temperature is 20 ^{o}C and the outdoor air temperature is -20 ^{o}C. Assume further that the average temperature of the rotor changes only 5 ^{o}C. The temperature profile in the rotor material does only change with a small amount per revolution in comparison with the temperature difference between the cold and hot side of the rotor. The high efficiency would not have been obtained if the temperature changes had been large in the rotor. The heat flow to the outdoor air is then proportional to

$$q\,(20-(-20))\,0.75$$

The heat flow through the rotor from the exhaust sector to the outdoor sector is proportional to

$$k\,q\,5$$

This gives

$$k_{max} = 6$$

The time unit can be estimated as follows. At maximum revolution speed (10 r/min) the whole temperature capacity C will be exchanged in 3 seconds. This gives the following relation

$$\frac{C}{k_{max}\,q} = 3 \text{ sec}$$

$$\frac{C}{q} = 18 \text{ sec} \qquad (k_{max} = 6)$$

The earlier chosen time unit is then estimated to 18 seconds. The questions then asked are:

How does the efficiency in steady state depend on the revolution speed?

How does the dynamics of an enthalpy exchanger depend on the revolution speed?

The efficiency e in steady state is computed by setting

$$\dot{x}_1(t) = 0.$$

$$\dot{x}_2(t) = 0.$$

$$u_1(t) = 0.$$

$$u_2(t) = 1.$$

in equations 3.3. and 3.4. The state $x_1(t)$ tells then how much of the heat that has been utilized by the exchanger. The efficiency can only be less than or equal to 1/2 in this model. The real process is a counter current heat exchange process. This properity cannot be built into this second order model.

If two compartment models are coupled in cascade, then the counter current properity can be built into the model. This means that the rotor is divided into two rotors. The "revolution flow" is now kq/2 per rotor and the heat capacity is also divided to C/2. The maximum efficiency is in this case equal to 2/3. The efficiency as a function of the revolution speed and the number of compartment models in cascade is shown in figure 3.2 and 3.3. The calculations are given in detail in appendix 1. The efficiency curves show that the process gain or the slope of the efficiency curves varies considerably. The process gain varies with a factor about 40. It is then diffi-

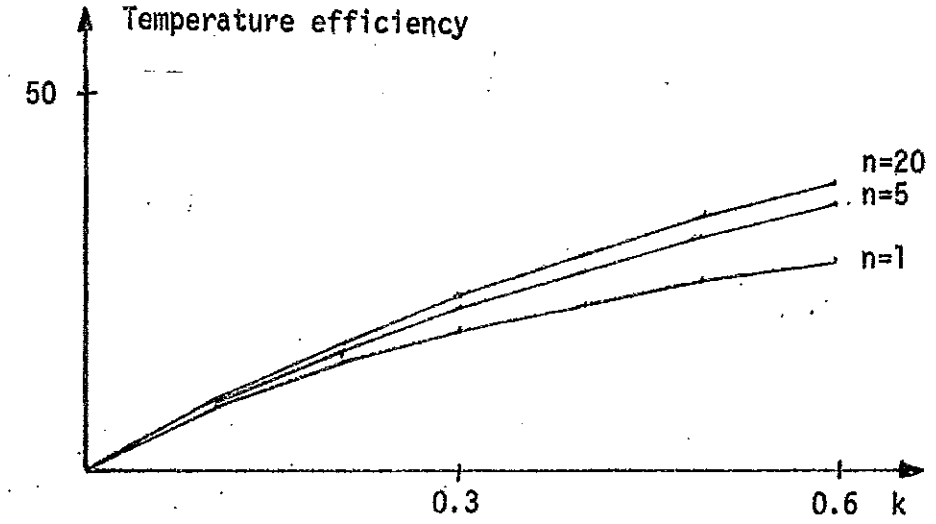

Figure 3.2 Temperature efficiency as a function of k and the number of models in cascade n.

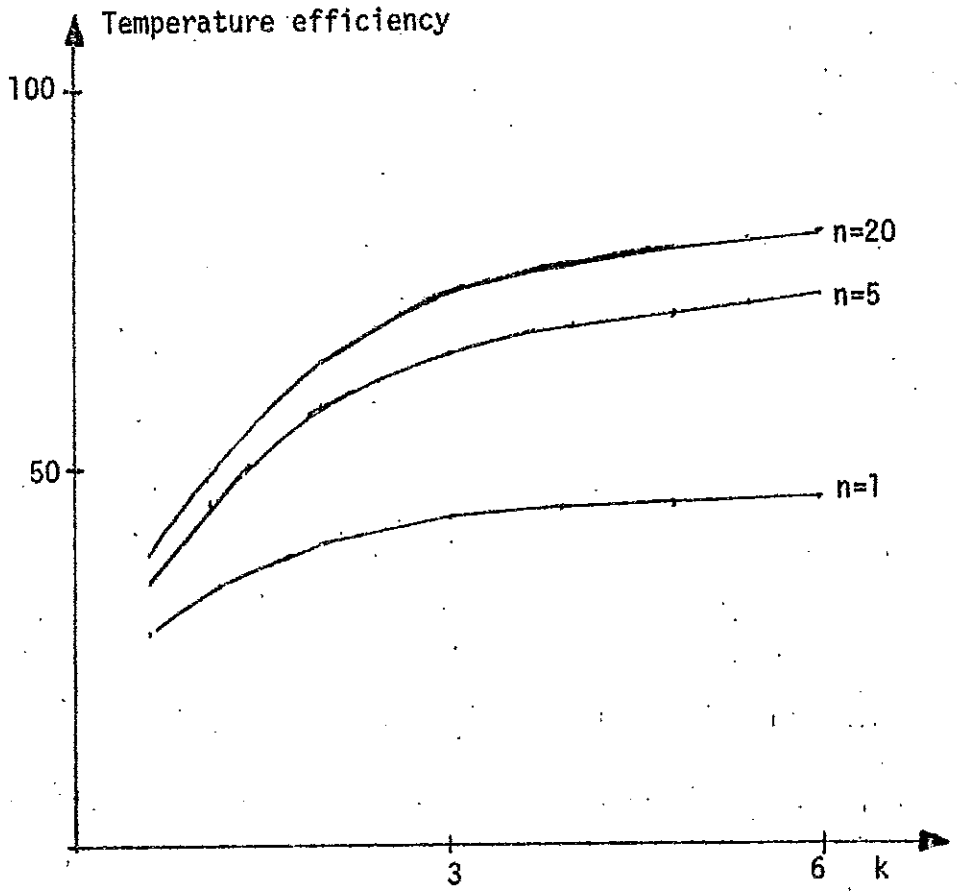

Figure 3.3 Temperature efficiency as a function of k and the number of models in cascade n.

cult to control the efficiency by controlling the revolution speed using a linear controller.

The dynamics as a function of the revolution speed can partly be studied by the eigenvalues of the matrix A below. This matrix is the system matrix to the equations (3.3) and (3.4).

$$A = \begin{bmatrix} -k-1 & k \\ k & -k-1 \end{bmatrix}$$

The eigenvalues are

$$\lambda_1 = -1$$

$$\lambda_2 = -1-2k$$

The second eigenvalue depends heavily on k. The variation of the parameter k from 0 to 6 has been determined earlier. The second eigenvalue will then vary from -1 to -13.

The time unit has earlier been estimated to about 18 seconds. This together with the eigenvalues shows that the time constants of the enthalpy exchanger are always less than 20 seconds.

This simple model has been divided in axial direction. Another possibility would be to divide the model in angular direction. This means that several compartments are coupled together as a circle. The flow kq goes from compartment to compartment in the circle. The exhaust air passes one half of the compartments and the outdoor air the other half.

3.2 A sector element model

The former model has been divided in axial direction. This was done so that the efficiency could become greater than 50% at high revolution speeds and thereby describing the temperature gradient in axial direction in the rotor. The temperature gradient will be more dominant in angular direction than in axialdirection at low revolution speeds. The rotor will be completely reloaded or unloaded before it leaves the exhaust respectively outdoor aur sector.

A simple model of a sector element of the rotor is considered.

The sector element follows the rotor in the rotation. This model can now be said to be distributed in angular direction and lumped in axial direction.

The following assumptions are made:

1 The temperature of the rotor material is assumed the same in the whole sector element.

2 The temperature of the air is assumed the same in the whole sector element.

3 The heat transfer between the air and the rotor material in the sector element is assumed to be proportional to the temperature difference.

Two simple heat balance equations can be given for the air temperature and the rotor material in this rotor sector. This model models a heat transfer process between two masses. The fact that these masses are rotating has no significance. The equations are as follows:

$$C_1 \dot{x}_1(t) = Ah(x_2(t)-x_1(t))+nC_1(u(t)-x_1(t)) \qquad (3.5)$$

$$C_2 \dot{x}_2(t) = Ah(x_1(t)-x_2(t)) \qquad (3.6)$$

This sector element will pass the exhaust air, the purging and the outdoor air sector.

The input u(t) is then either the exhaust air, the purging air or the outdoor air temperature. The exhaust temperature is assumed to be 1 ^{o}C and the outdoor air temperature is assumed to be 0^{o}C. The input u(t) can then be given as follows:

$$u(t) = \begin{cases} 1 & 0 \leq t \leq t_1 \\ u_m & t_1 \leq t \leq t_2 \\ 0 & t_2 \leq t \leq t_4 \end{cases} \qquad (3.7)$$

The cleaning air temperature u_m is the average value of the airtemperature $x_1(t)$ in (t_2,t_3). This gives

$$u_m = \frac{\int_{t_2}^{t_3} x_2(t)\,dt}{t_2 - t_1} \qquad (3.8)$$

The steady state solution is found by numerical solution of the equations (3.5) and (3.6). The temperature efficiency, e, is the ratio between the average temperature of the heated outdoor air and the average temperature of the exhaust air, i.e.

$$e = \frac{\int_{t_3}^{t_1} x_1(t)\,dt}{\int_{0}^{t_1} u(t)\,dt} \qquad (3.9)$$

The values u_m and e can be computed by defining a new state variable $x_3(t)$.

$$\dot{x}_3(t) = x_1(t) \tag{3.10}$$

Now we get

$$u_m = \frac{x_3(t_3)-x_3(t_2)}{t_2-t_1} \tag{3.11}$$

and

$$e = \frac{x_3(t_4)-x_3(t_3)}{t_1} \tag{3.12}$$

What are the values on C_1, C_2, A, h and n for the actual enthalpy exchanger? The rotor volume is

$$V_{12} = 0.2 \cdot \overline{11} \cdot 0.95\ m^2 = 0.57\ m^3$$

The rotor volume consists of 80% air. This gives

$$V_1 = 0.8 \cdot V_{12} = 0.45\ m^3$$
$$V_2 = 0.2 \cdot V_{12} = 0.11\ m^3$$

and

$$C_1 = 0.45 \cdot 1.29 \cdot 1000 = 580\ J/^oC$$

The heat capacity of the rotor material is assumed to be 4000 J/kg ^oC. This gives

$$C_2 = 440000\ J/^oC$$

The exhaust and outdoor air flows are together 10 m^3/sek. This gives:

$$n = \frac{10}{V_1} = 22.2 \text{ sec}^{-1}$$

The surface per volume rotor is about 3000 m^2/m^3. This gives

$$A = 1700 \text{ m}^2$$

The heat transfer coefficient h $W/m^2\ ^oC$ varies from 10 $W/m^2\ ^oC$ to 100 $W/m^2\ ^oC$ at forced ventilation. A value of 30 $W/m^2\ ^oC$ will be used. This gives

$$Ah = 51000 \text{ W/}^oC$$

The whole purging sector is assumed to be 10.8 ^oC. The equations (3.5), (3.6) and (3.10) have been simulated with the given constants for revolution speeds 0.1(0.1)1.0 r/min. The temperature efficiency is given in table 3.1.

This model can also be used to study dynamic properities. Several sector element model have then to be used together. The equations are nonlinear if revolutions speed changes are studied.

One remark about this sector model is that the temperature efficiency will always be less than 50%. The temperature efficiency can be higher if the sector element is divided in axial direction.

Table 3.1 Temperature efficiency in percent as a function of revolution time T in seconds for the sector element model for different heat capacity C in kJ/^{o}C and heat transfer conductance Ah in kW/^{o}C. The cleaning sector angle is 10.4^{o}.

C	22	22	44	44
Ah	17	51	17	51
T				
6.	27.7	38.8	27.8	39.0
7.5	27.6	38.6	27.7	39.0
10.	27.4	38.2	27.7	38.9
15.	27.0	37.2	27.6	38.6
30.	25.2	32.9	27.0	37.2
60.	20.1	23.2	25.1	32.9
120	11.8	11.8	20.1	23.2
600	3.7	3.3	9.3	8.9
1200	1.1	0.8	3.7	3.3

4 Models based on experimental data

In section 3 different models were constructed to study static and dynamic properities of the process. This is also possible to do by using experimental data. Measurements of temperatures and revolution speed can be made. The revolution speed has to be controlled in the experiments in order to obtain suitable data.

In section 4.1 the measurement and control equipment are described. Two different types of experiment are made. In section 4.2 the temperature efficiency is determined as a function of the revolution speed with experimental data. In section 4.3 the dynamic properities are studied at different revolution speed levels with experimental data. In section 4.4 the alaizing effect at startup is shown.

4.1 Measurement and control equipment

Three dry air temperatures were measured (exhaust air before enthalpy exchanger $u_2(t)$, outdoor air before $u_1(t)$ and after enthalpy exchanger $y(t)$). Thermistors were used as temperature sensors.

Three sensors were used to measure the outdoor air temperature after the enthalpy exchanger. This was done because of the large temperature gradients variation in the air stream. The mean value of these three temperatures was used as outdoor air temperature after enthalpy exchanger $y(t)$. The location of the temperature sensors are given in figure 4.2.

The revolution speed of the rotor was not measured directly. The motor speed was measured instead. A tachometer was used. The signal was filtered by a RC filter (RC = 0.4 sec).

The tachometer has been calibrated and the result is shown in figure 4.3. Another calibration has been made between the rotor revolution speed and the tachometer signal. Ten revolutions took 68 seconds at maximum speed and the tachometer signal was 8.6 volt. The maximum revolution speed is then 8.8 r/min. The number of revolutions per minute is then almost equal to the measured revolution speed signal $u_3(t)$ in volts.

The revolution speed is controlled. The sum of the measured tachometer signal $u_3(t)$ and the revolution command signal $u_4(t)$ are fed into a electronic circuit. The signal $u_4(t)$ has the opposite sign of the signal $u_3(t)$. This electronic circuit transforms the sum or the errorsignal to a pulselength modulated three state signal (forward, idle, backward). This signal controls a motor potentiometer. This potentiometer controls the rotor motor moment and thereby the revolution speed. The moment of inertia of the rotor will introduce dynamic between the motor potentiometer and the revolution speed.

A coupler/controller system (Hewlett Packard) has been used as a process interface to measure analog inputs and to control analog and logical outputs. The c/c is interfaced to a PDP-15 process computer (Digital). Details about the c/c system are given in Jensen (1973). Lowspeed modems (200 baud) were used as communication line between the process in the office building of the Swedish Steam Users' Association at Malmö and process computer at the Division of Automatic Control, Lund Institute of Technology.

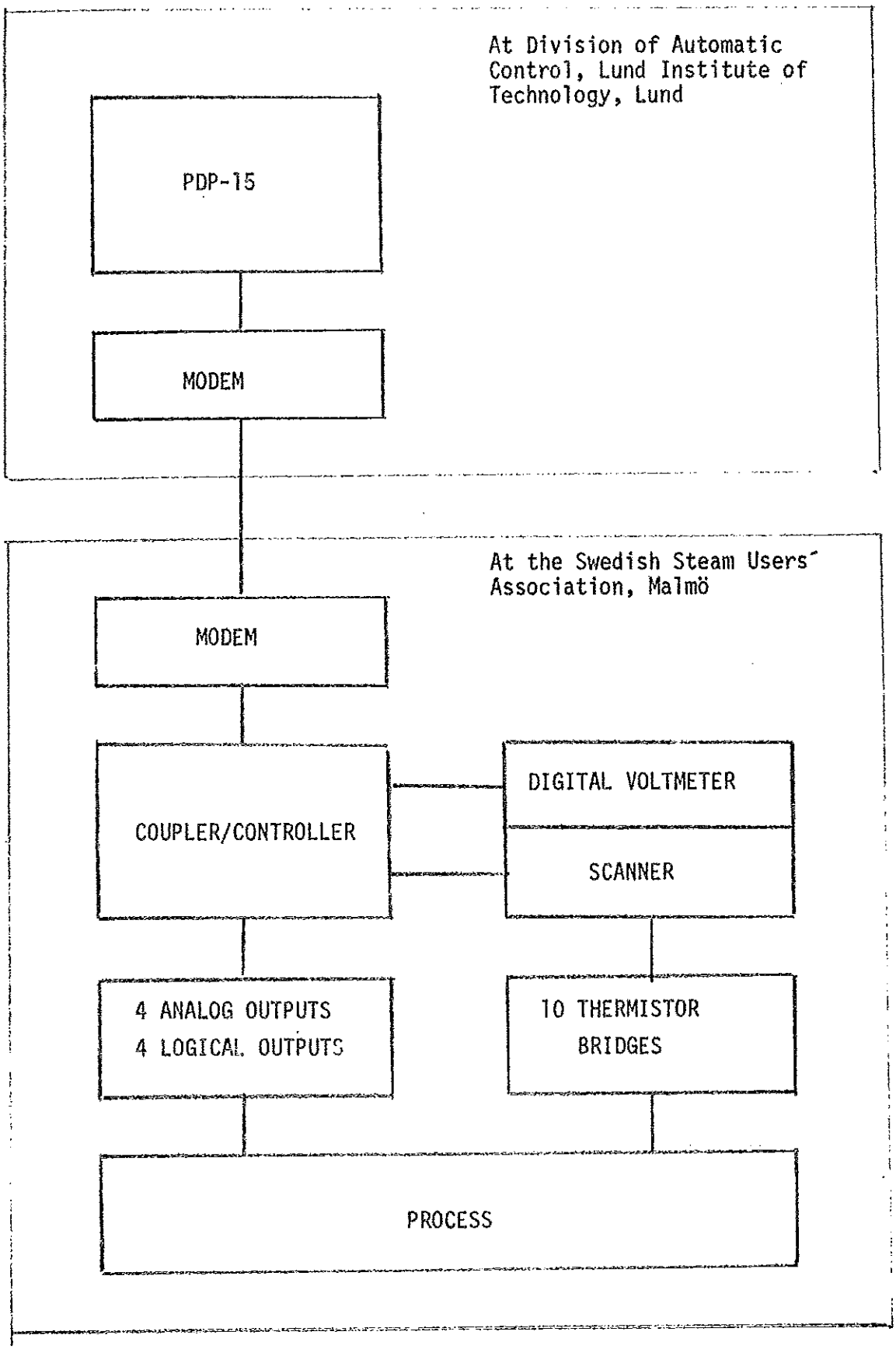

Figure 4.1 Plant and equipment

from the side

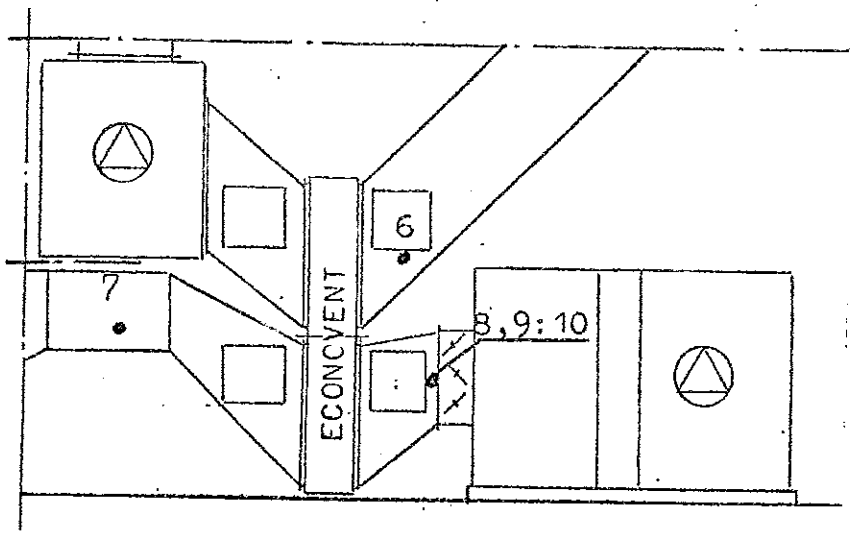

from above

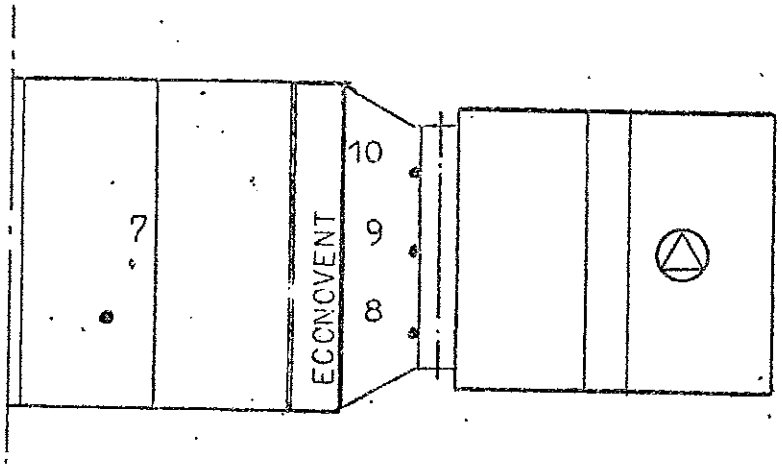

Figure 4.2 Enthalpy exchanger with inlet and outlet air fans and location of temperature sensors.
Scale 1:50

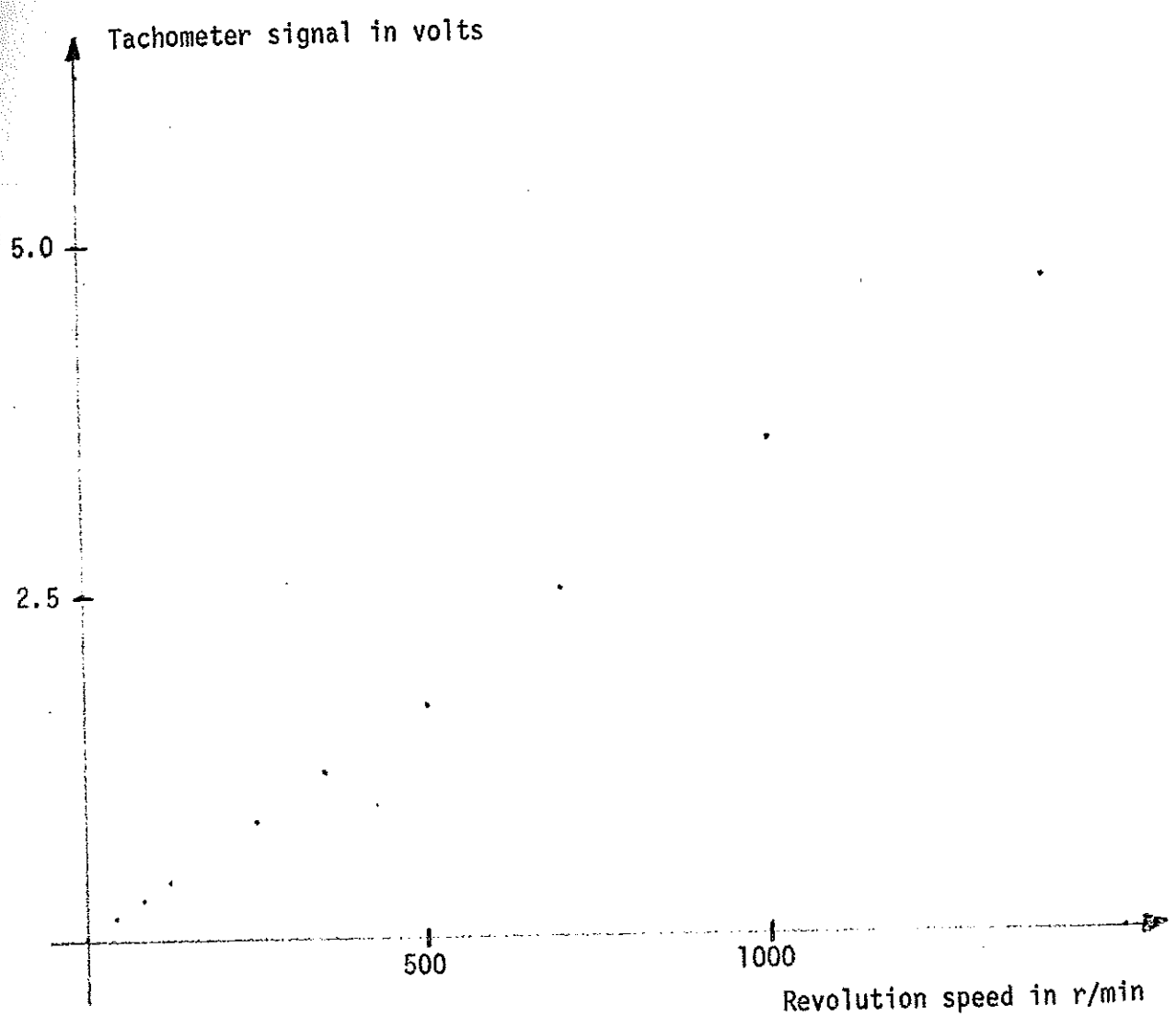

Figure 4.3 Calibration curve of tachometer

4.2 Determination of temperature efficiency using experimental data

Experiments have been made straightforwardly. The rotor revolution speed command signal $u_4(t)$ has been held constant on 25 different levels during 15 minutes. The sampling interval has been 20 seconds. The whole experiment is shown in figure 4.4. Samples 21 to 40 of each level have been used to compute mean values of every level. These mean values have been used to compute the temperature efficiency e as follows

$$e = \frac{y - u_1}{u_2 - u_1}$$

The temperature efficiency e is given as a function of the tachometer signal u_3 in figure 4.5 and 4.6. The used mean values of u_1, u_2, u_3, u_4 and y are given in table 4.1. The temperature efficiency as a function of the revolution speed signal in figure 4.5 and 4.6 is simular to the manufacture's curve in figure 2.4 and also simular to the theoretic curves in figure 3.2 and 3.3.

The nonlinearity has been found to vary with about 10% to 15% at revolution speeds below 1 r/min, when preliminary control experiments were carried out. The variations can be explained by different amount of water in the rotor. This will give the rotor different heat capacity. Further the enthalpy exchange is close to zero at low revolution speeds, but this does not ensure that the temperature efficiency and the moisture efficiency is close to zero. Instead the two airstreams can change their temperature and moisture and still keep their enthalpy constant. This means that one airstream is humidified and the other is dehumidified. Both the vaporization heat and the dissolving heat are disengaged, when water vapour in the air is transferred into the rotor material. The temperature of the airstream is then raized and water content is reduced. The opposite is going on in the other airstream.

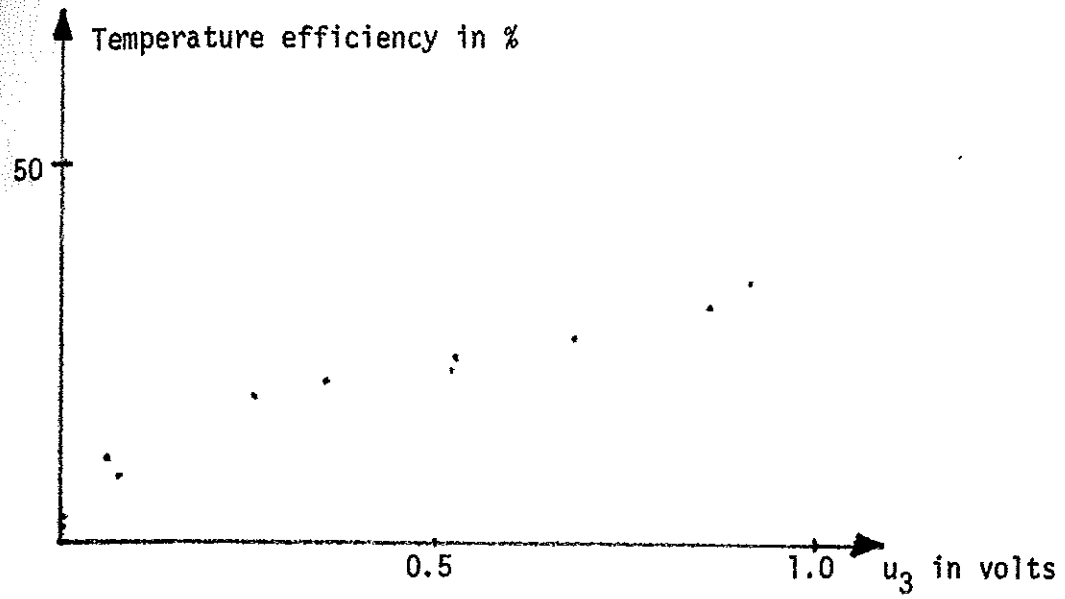

Figure 4.4 Measured temperature efficiency e in % as a function of revolution speed signal u_3 in volts from one experiment.

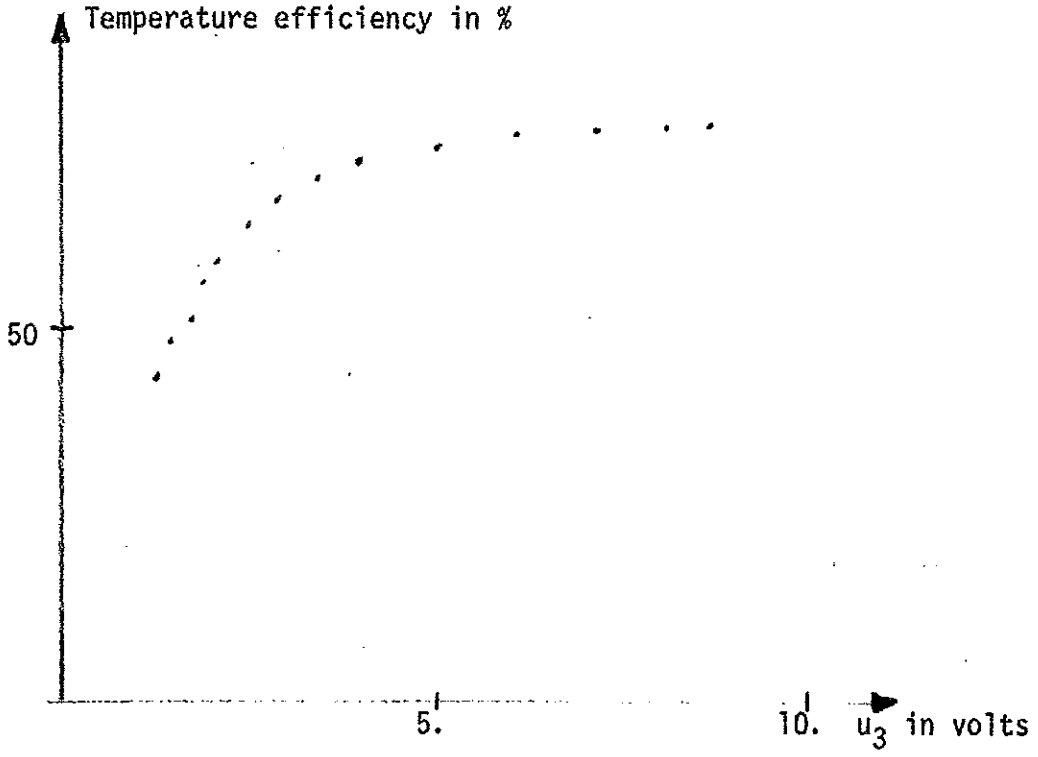

Figure 4.5 Measured temperature efficiency e in % as a function of revolution speed signal u_3 in volts from one experiment.

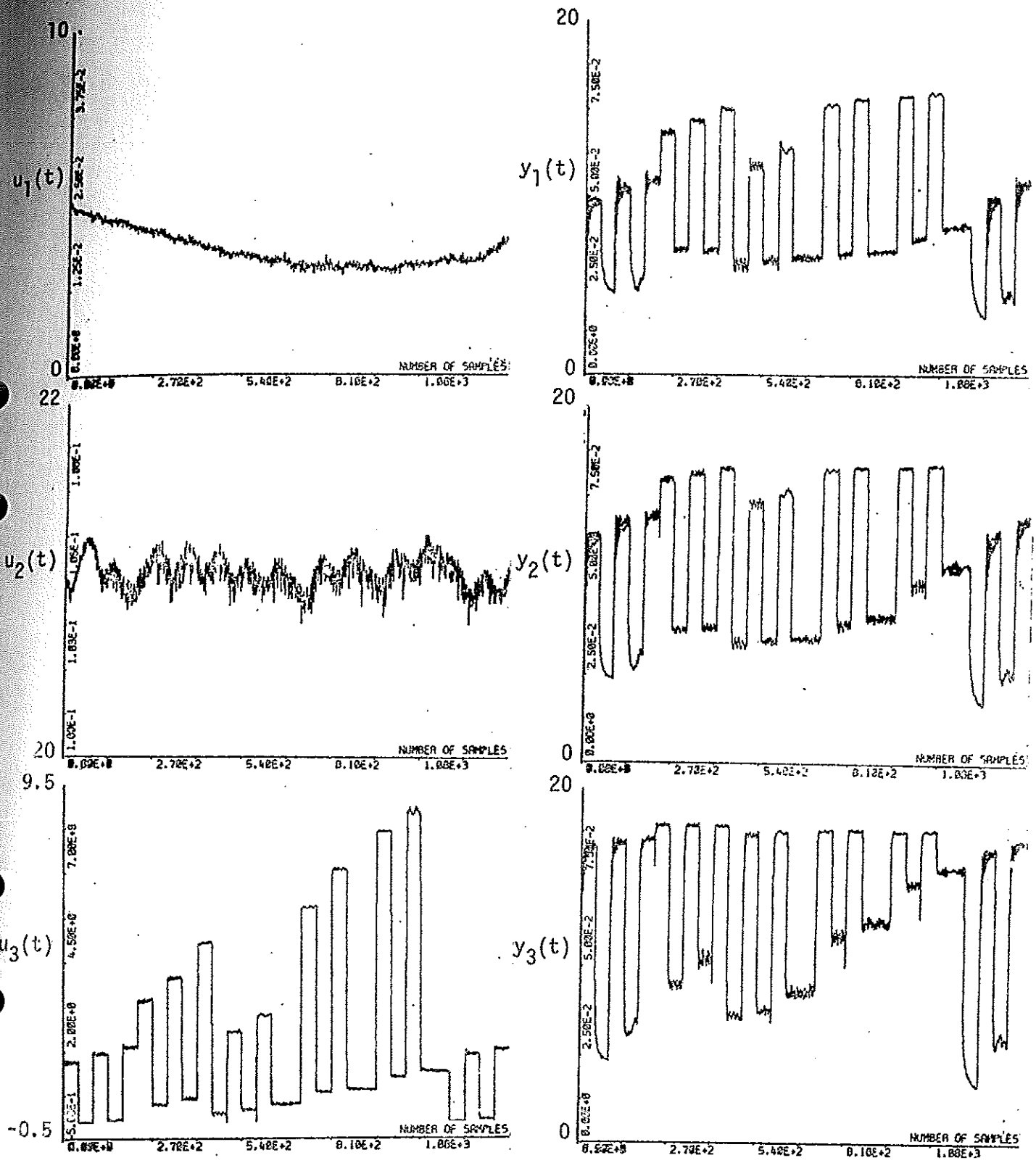

Figure 4.6 Static experiment

$u_1(t)$ outdoor air temperature in ^{o}C

$u_2(t)$ exhaust air temperature in ^{o}C

$u_3(t)$ measured revolution speed in volts

$y_1(t)$, $y_2(t)$ and $y_3(t)$ outdoor air temperature after enthalpy exchanger in ^{o}C

The whole experiment length is 450 minutes

Table 4.1 Mean values from temperature efficiency experiment shown in figure 4.4 in cronological order as they appear in figure 4.6.

$u_1(t)$ Outdoor air temperature in ^oC

$u_2(t)$ Exhaust air temperature in ^oC

$u_3(t)$ Revolution speed signal in volts

$u_4(t)$ Revolution speed command in volts

$y(t)$ Outdoor temperature after enthalpy exchanger in ^oC

$e(t)$ Temperature efficiency in %

$u_1(t)$ ^oC	$u_2(t)$ ^oC	$u_3(t)$ V	$u_4(t)$ V	$y(t)$ ^oC	$e(t)$ %
4.80	21.00	1.73	-1.57	13.01	50.64
4.63	21.21	0.00	0.00	4.96	1.97
4.48	21.01	1.96	-1.79	13.62	55.33
4.43	21.00	0.07	-0.09	5.76	8.01
4.24	20.93	2.16	-1.98	14.02	58.60
4.13	21.07	3.45	-3.49	15.88	69.37
4.05	21.10	0.51	-0.48	7.88	22.46
3.87	21.04	4.08	-3.97	16.20	71.82
3.79	21.11	0.68	-0.58	8.42	26.75
3.63	21.05	5.06	-4.97	16.49	73.87
3.49	21.09	0.25	-0.19	6.82	18.94
3.42	21.00	2.57	-2.47	14.64	63.80
3.36	21.03	0.35	-0.28	7.05	20.87
3.25	20.97	3.01	-2.98	15.23	67.58
3.26	21.02	0.51	-0.38	7.45	23.62
3.09	20.94	0.52	-0.67	7.49	24.66
3.07	20.93	6.06	-5.99	16.48	75.09
3.12	21.06	0.86	-0.77	8.87	32.07
3.02	21.03	7.12	-6.98	16.64	75.62
3.10	21.11	0.93	-0.89	9.30	34.41
3.12	21.01	0.93	-0.99	9.30	34.58
3.02	21.00	8.17	-7.98	16.70	76.09
3.08	21.09	1.28	-1.18	10.90	43.43
3.13	21.08	8.74	-8.97	16.80	76.15
3.17	21.15	1.46	-1.38	11.70	47.44
3.28	21.09	1.45	-1.57	11.76	47.65
3.26	21.02	0.00	0.00	3.79	2.95
3.24	20.92	1.93	-1.79	13.05	55.51
3.45	20.99	0.06	-0.09	5.34	10.77
3.74	20.96	2.07	-1.98	13.84	58.68

4.3 Dynamic models based on experiments

To obtain dynamic models a special experiment has been made. The revolution command signal $u_4(t)$ has been varied around 6 different levels with different amplitudes. A PRBS (Pseudo Random Binary Sequence) signal determined the sign of the amplitude. Details about PRBS can be found in Davis (1970). The sampling interval was 20 seconds. The number of samples per level was 225. The basic period T of the PRBS signal was 5 minutes or 15 samples. The order of the PRBS signal n was 4. The total PRBS signal period length was 75 minutes or 225 samples ($= 15 \cdot (2^4-1)$).

The measured revolution speed $u_3(t)$ and the five different temperatures are shown in figure 4.7.

The dynamics from outdoor air temperature $u_1(t)$, exhaust air temperature $u_2(t)$ and revolution speed signal $u_3(t)$ to the outdoor air temperature after the enthalpy exchanger $y(t)$ was modelled as follows. The coefficients of a first order difference equation

$$y(t) + a\, y(t-1) = b_1\, u_1(t-1) + b_2\, u_2(t-1) + b_3\, u_3(t-1) + v(t)$$

were determined using a least squares criterion. The model parameters a, b_1, b_2 and b_3 are thus found by minimizing the loss function

$$V = \sum_{t=1}^{N} v(t)^2$$

Further details about the method are given in Aström (1968).

The revolution speed servo dynamics are excluded in the pro-

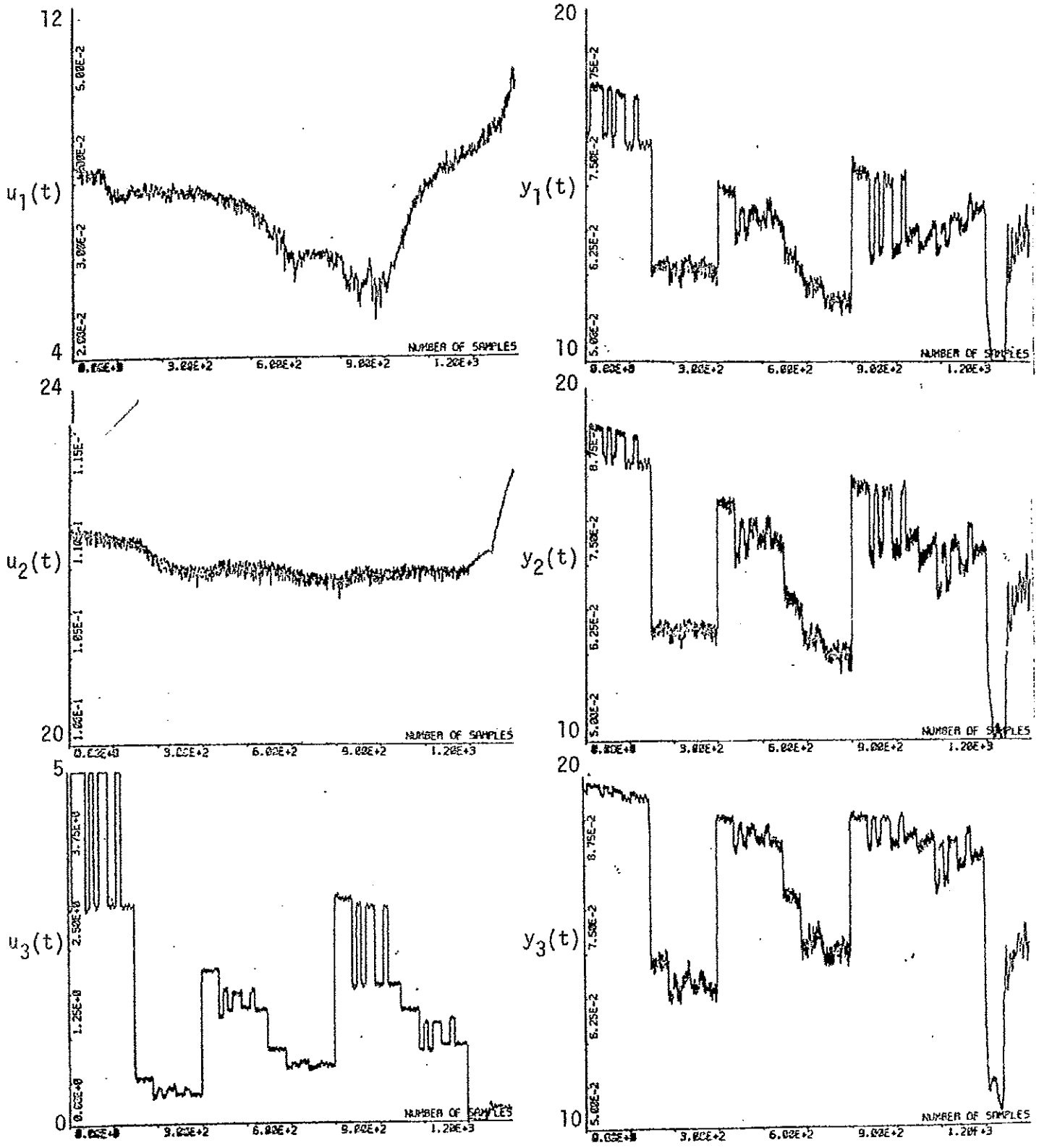

Figure 4.7 Dynamic experiment

$u_1(t)$ outdoor air temperature in ^oC

$u_2(t)$ exhaust air temperature in ^oC

$u_3(t)$ measured revolution speed in volts

$y_1(t)$, $y_2(t)$ and $y_3(t)$ outdoor air temperature after enthalpy exchanger in ^oC

The whole experiment length is 500 minutes

cess model by using the measured revolution speed signal as input.

Four different models are studied.

Model	Identified parameters	Fixed parameters
1	a b_3	$b_1 = b_2 = 0$
2	a b_2 b_3	$b_1 = 0$
3	a b_1 b_3	$b_2 = 0$
4	a b_1 b_2 b_3	-

The identification results are shown in table 4.2 for model 1 and 4 and for revolution speed command signals $u_4(t)$.

Table 4.2 First order model parameters and e_{std} the standard deviation of model error v(t) for models 1 and 4 and different revolution command signals $u_4(t)$.

Command signal $u_4(t)$ level	amplitude	Model parameters a	b_3	b_2	b_1	e_{std}
0.5	0.2	-0.429	1.001	-	-	0.092
		-0.325	1.574	-0.101	-0.489	0.085
0.85	0.15	-0.608	2.054	-	-	0.1603
		-0.548	2.089	0.035	0.651	0.1568
1.25	0.25	-0.860	0.163	-	-	0.1601
		-0.327	1.357	0.596	0.210	0.1248
1.75	0.25	-0.219	1.302	-	-	0.1073
		-0.220	1.363	-0.096	0.036	0.1056
2.50	0.50	-0.280	0.849	-	-	0.1524
		-0.070	1.130	0.294	-0.166	0.1259
4.0	1.0	-0.532	0.207	-	-	0.0925
		-0.138	0.340	0.327	0.407	0.0585

The dynamic is very fast. The model parameter a_1 is usually greater than -0.5. This value corresponds to continuous time conctant less than 30 seconds.

The static gain g between the output the outdoor air temperature after the enthalpy exchanger y(t) and the revolution speed signal $u_3(t)$ can be computed as $g = b_3$ with $(1+a_1)$. The model parameters are given in table 4.3. This is done for all the models and the results are given in table 4.3. The static gain varies from 0.39 to 5.24 ^{o}C/volts or with a factor of 13.5.

Table 4.3 The static gain g between the output y(t) and the third input $u_3(t)$ for models 1 and 4 and different revolution speed command signals $u_4(t)$.

Command signal $u_4(t)$		Static gain for model	
level	amplitude	1	4
0.50	0.2	1.75	2.34
0.85	0.15	5.24	4.73
1.25	0.25	1.16	2.01
1.75	0.25	1.66	1.75
2.50	0.50	1.18	1.21
4.00	1.00	0.44	0.39

4.4 Startup fenomena

An effect that cannot be described by the simple models in section 3 has been found. When the revolution speed has been zero for a certain amount of time then the outdoor air temperature after the enthalpy exchanger oscillates when a step is introduced in the revolution speed. This is due to the fact that one half of the rotor is hot and the other half is cold.

Three examples are shown in figure 4.8. The measured period time of the oscillating output y(t) is 250 sec, 140 sec and 400 sec. The measured revolution period time is 270 sec, 11.5 sec and 12.4 sec. The used sampling intervals have been 30 sec, 20 sec and 20 sec. The figures above show that another effect, the aliazing effect, also occurs. The measured period time of the oscillating output y(t) is a multiple of the real period time. This gives

$$n_1 = \frac{250}{270} = 0.925 \approx 1$$

$$n_2 = \frac{140}{11.5} = 12.2 \approx 12$$

$$n_3 = \frac{400}{12.4} = 32.2 \approx 32$$

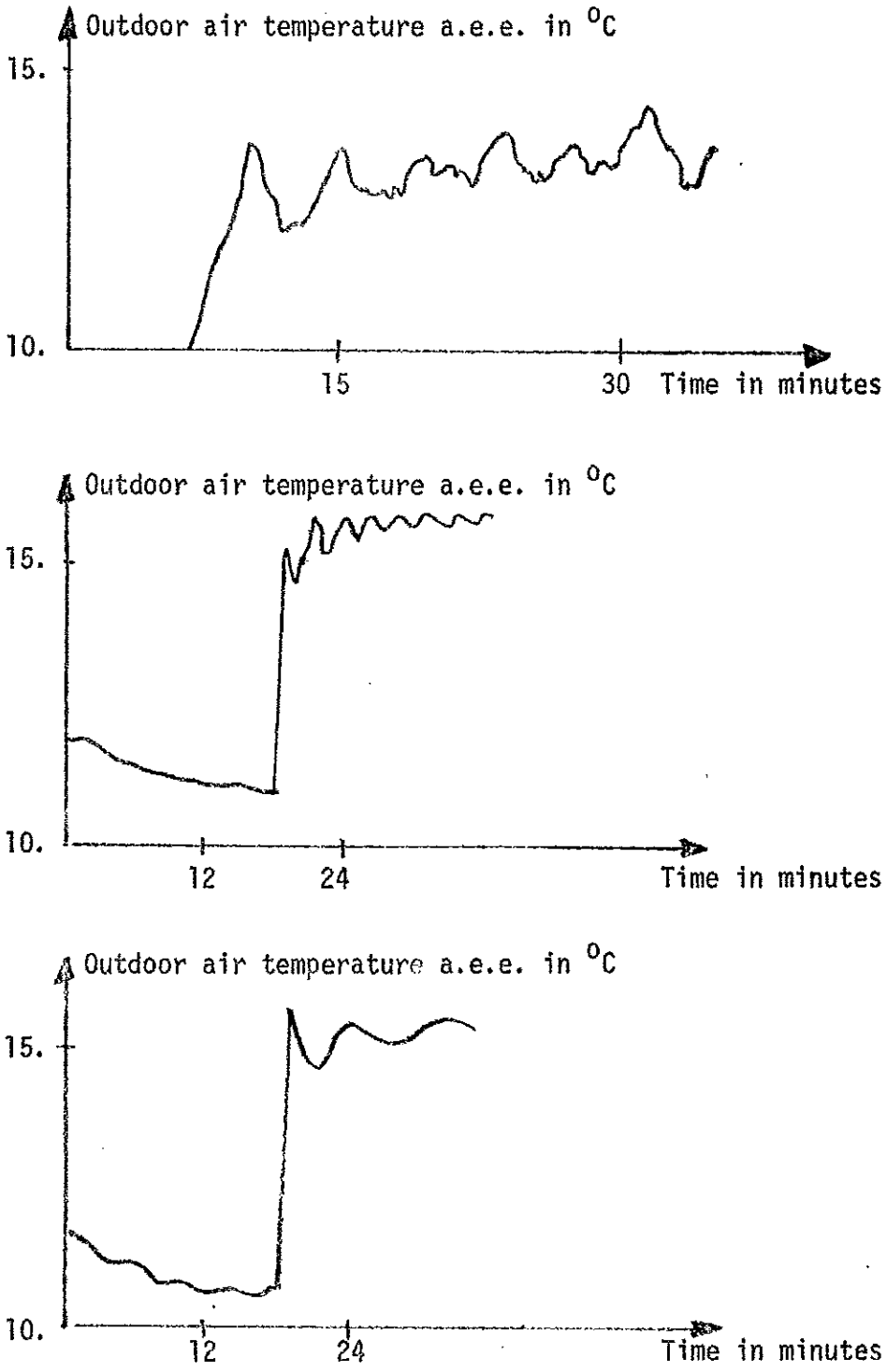

Figure 4.8 Examples of start and aliazing effects

5 Determination of a regulator

In section 3 and 4 static and dynamic properities have been studied. Based on this knowledge a regulator will be determined in this section. Only digital controllers for temperature control will be considered.

5.1 Background

The control problem is to keep the air temperature after the enthalpy exchanger constant (denoted $y(t)$). The control signal can be the revolution speed command signal (denoted $u_4(t)$) to the revolution speed servo. The position change signal to the motor potentiometer is the other possible control signal. The motor potentiometer controls the drive motor moment and thereby the revolution speed (denoted $u_3(t)$). The disturbances are the outdoor and the exhaust air temperature (denoted $u_1(t)$ and $u_2(t)$). These are supposed to be available.

There are several things that should be kept in mind when designing a regulator for an enthalpy exchanger.

- The temperature efficiency as a function of the revolution speed is very nonlinear.
- This nonlinearity varies with the outdoor climate.
- The total process gain between $y(t)$ and $u_3(t)$ depends also on the temperature difference between exhaust and outdoor air ($u_2(t) - u_1(t)$).
- The dynamics is rather fast for revolution speeds above 0.5 r/min.
- The revolution speed can be controlled from 0.5 r/min to 10 r/min. Lower revolution speeds will be difficult to handle.

- The revolution speed $u_3(t)$ can vary due to that the rotor is unbalanced. This can be the case after a stand still.

- The aliazing effect should also be taken into account. This effect occurs when the time for one revolution is less than two samplings intervals. This effect can be observed if the revolution speed has been zero or close to zero. When the revolution speed is increased then the output y(t) will oscillate with a frequence equal to the revolution frequence. This frequence will be equal to a multiple of the observed frequence.

- The average temperature must be measured. There are large temperature gradients in the cross section of the air duct after the enthalpy exchanger.

- The average temperature can also be measured after the air has been mixed after the filter and the inlet air fan. However the fan will increase the temperature with about 1 ^{o}C to 2 ^{o}C. Some dynamic will also be added to the total system.

A straight forward solution of the control problem would be to determine the nonlinearity and to use it to compute the desired revolution speed. However the nonlinearity varies, which makes it uncertain to use this approach of the control problem.

An integral can be included in the regulator in order to compensate for the varing nonlinearity. Variations of the slope of the nonlinearity cannot be eleminated. The closed loop gain can then vary and make the process unstable.

Another solution would be to identify the efficiency curve in the actual working point as follows

$$e(t) = k\, u_3(t) + 1 \qquad (5.1)$$

where e(t) is the efficiency, k and l are constants, which have to be determined. The desired revolution speed $u_4(t)$ can then be computed from the identified model, measured and desired temperatures. The model (5.1) is a static model. The process can almost be considered as a static process if the sampling interval is one minute or larger.

A more direct approach of the control problem would be to directly identify model parameters in a model between the output y(t), the outdoor air temperature after enthalpy exchanger and the input $u_3(t)$ the measured revolution speed. The model parameters k and l would then have to track variations in the outdoor and exhaust air temperature. The input $u_3(t)$ and the output y(t) can become uncorrolated. This gives bad model parameters and thereby also a bad control signal.

In the model (5.1) the input can be the measured revolution speed $u_3(t)$ or the revolution command signal $u_4(t)$. Uncontrollable revolution speed variations can make the output e(t) and the input $u_4(t)$ uncorrolated. The best input would then be the measured revolution speed signal $u_3(t)$.

5.2 A selftuning regulator

The computations that takes place in the selftuning regulator can be summarized as follows:

1 get the new measurements
$u_1(t)$, $u_2(t)$, $u_3(t)$ and $y(t)$

2 compute the actual efficiency

$$e(t)=(y(t)-u_1(t))/(u_2(t)-u_1(t)) \qquad (5.2)$$

3 The measurements $e(t)$, $e^2(t)$, $u_3(t)$, $u_3^2(t)$ and $e(t)u_3(t)$ are weighted in time so that old measurements are forgotten. This is done by using a forgetting factor λ as follows

$$S(e,t)= \lambda\, S(e,t-1)+(1-\lambda)\, e(t) \qquad (5.4)$$
$$S(e,0) = 0$$

where

$$0 \leq \lambda \leq 1$$

Further details are given in Wieslander (1969)

4 compute the parameters k and l to the line (5.1) using the values obtained in point 3

5 compute the desired efficiency

$$e_{set}=(y_{set}-u_1(t))/(u_2(t)-u_1(t)) \qquad (5.3)$$

6 compute the new revolution speed command signal $u_4(t) = -(e_{set}-l)/k$ (notice that $u_4(t)$ has the opposite sign of $u_3(t)$)

The rest of this section will only deal with point 4.

The line (5.1) with the parameters k and l is fitted to the measurements e(t) and $u_3(t)$ so that a function V(k,l) is minimized. The function V(k,l) is the sum of the squares of the orthogonal distances between the line and the measurements. The orthogonal distance is used because both measurements are uncertain and the slope varies considerably with the working point. This is not the case in the normal least squares method. The vertical distance is used. The function V(k,l) can be written as follows

$$V(k,l) = \sum_{i=1}^{N} \lambda^{2(N-i)}\, d^2(k,l,e(i),u_3(i)) \qquad (5.5)$$

where $d(k,l,e(i),u_3(i))$ is the orthogonal distance between the line (5.1) and the point $(e(i), u_3(i))$. How the distance function is obtained is shown in appendix 3. N is the number of observations.

The function V(k,l) can also be written as follows using the timeweighted mean values when the second argument is left out.

$$V(k,l) = \frac{N}{(k^2+1)} (S_{e^2} + k^2 S_{u_3^2} + l^2 - 2k S_{eu_3} - 2 l S_e + 2 kl S_{u_3}) \qquad (5.6)$$

The function V(k,l) is differentiated with respect to k and l to find the minimum of V(k,l).

$$\frac{\partial V}{\partial k} = \frac{2N}{(k^2+1)^2} (k S_{u_3^2} + (k^2-1) S_{eu_3} - k S_{e^2} - -(k^2 l-l) S_{u_3} + 2 kl S_e - kl^2) \qquad (5.7)$$

$$\frac{\partial V}{\partial k} = \frac{2N}{(k^2+1)} (k\, S_{u_3} - S_e + 1) \tag{5.8}$$

A necessary condition for a minima are

$$\frac{\partial V}{\partial k} = 0 \tag{5.9}$$

$$\frac{\partial V}{\partial 1} = 0 \tag{5.10}$$

The parameter 1 is eliminated in equation (5.9) by using equation (5.10). This gives the following equation in k.

$$k^2 + 2\,pk - 1 = 0 \tag{5.11}$$

where

$$p = (S_{u_3^2} - (S_{u_3})^2 + (S_e)^2 - S_e^2)/2\,(S_{eu_3} - S_e S_{u_3}) \tag{5.12}$$

The denominator in expression (5.12) can become close to zero or zero. This is the case when e(t) and $u_3(t)$ are uncorrolated.

One pair (k,1) gives the real minima and the other pair is a stationary point. The values of the function V(k,1) can be computed for the two solutions so that the minimizing solution can be found.

The two lines $(k_1,1_1)$ and $(k_2,1_2)$ are orthogonal which means that they will have opposite signs. The sign of the wanted solution is usually known. The right solution can then be chosen by the sign.

A special case is when 1 is equal to zero. Now equation (5.12) becomes

$$p = (S_{u_3}^2 - S_e^2)/2\, S_{eu_3} \qquad (5.13)$$

Only three different expectation values are needed.

The parameters k or l can also be determined in other special cases where k or l are fixed to a certain value or are a function of the other variable.

6 Full scale control experiments

6.1 Implementation of a selftuning regulator

The selftuning regulator has been implemented for the two cases

$$u_4(t) = -(e_{set} - l)/k$$

and

$$u_4(t) = -e_{set}/k$$

where e_{set} is the computed desired temperature efficiency value and $u_4(t)$ is the revolution speed command signal. The model parameters k and l are to be identified.

The sampling interval has been chosen to one minute. The command signal to revolution speed has been limited to (0.05,8.0) volts. A standstill of the rotor was to be avoided. The revolution speed was controlled by the process computer by positioning the motor potentiometer forward or backward. The sum between the setpoint $u_4(t)$ and the measured revolution speed $u_3(t)$ determined the time that the motor potentiometer should be moved. This was done so that the error was reduced and not totally eliminated. Revolution speed variations would otherwise have been excited. The revolution speed varies with about $\pm$0.05 r/min or $\pm$0.05 volts without control. The earlier used revolution speed control was not used. The aquaracy could not be made better than the used computer revolution speed servo.

The tachometer signal was in this case filtered with a time-constant T=RC=5 seconds.

The revolution speed changes were also limited. The selftuning regulator can generate very large or small control signal when it degenerates. The constant p in equation (5.12) is then close to infinity.

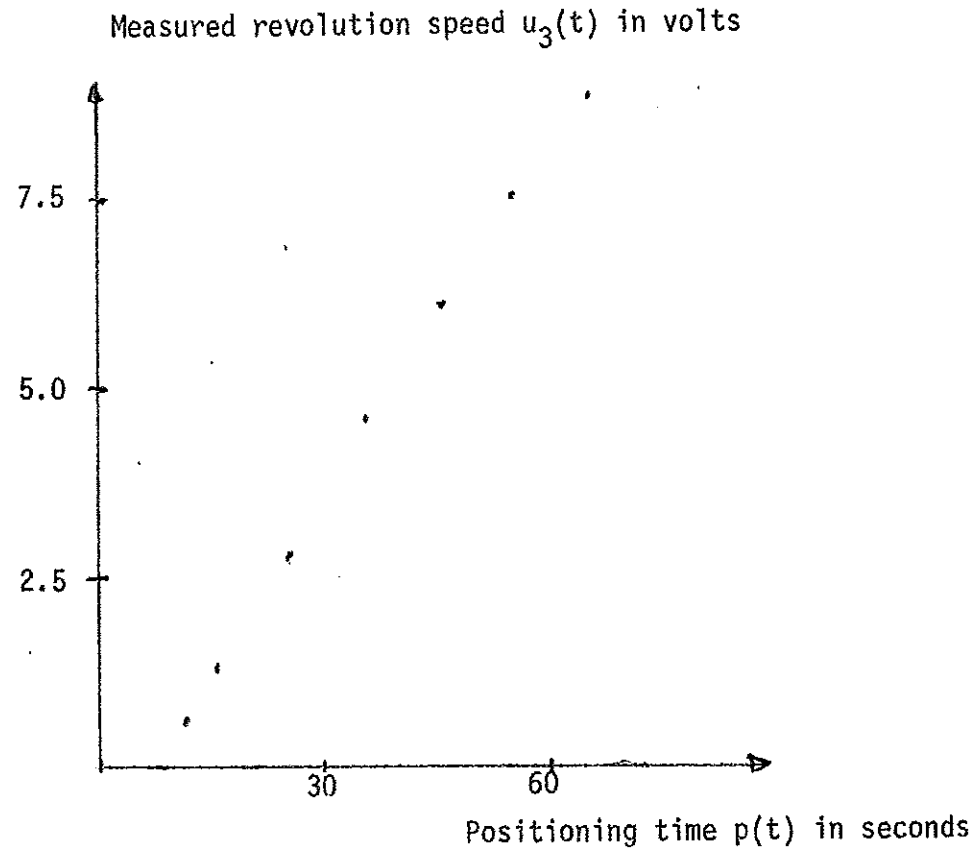

Figure 6.1 Measured revolution speed signal $u_3(t)$ in volts as a function of positioning time p(t) in seconds from stand still.

6.2 A selftuning regulator with one parameter

The regulator can be written as

$$u_4(t) = -e_{set}/k$$

where k is the parameter that is tuned. The regulator has been run on five different temperature efficiency levels (50%, 45%, 40%, 35% and 30%) and with four different forgetting factors (0.8, 0.6, 0.4 and 0.2). The efficiency has been changed every 30th minute. The forgetting factor has been changed every 120th minute. The desired temperature efficiency value has been converted into a corresponding temperature setpoint y_{set} at the start on each level. Each efficiency level has been run for 30 minutes or 30 samples. The result of the experiment is shown in figure 6.2 and 6.3. For later reference this implementation is denoted R1.

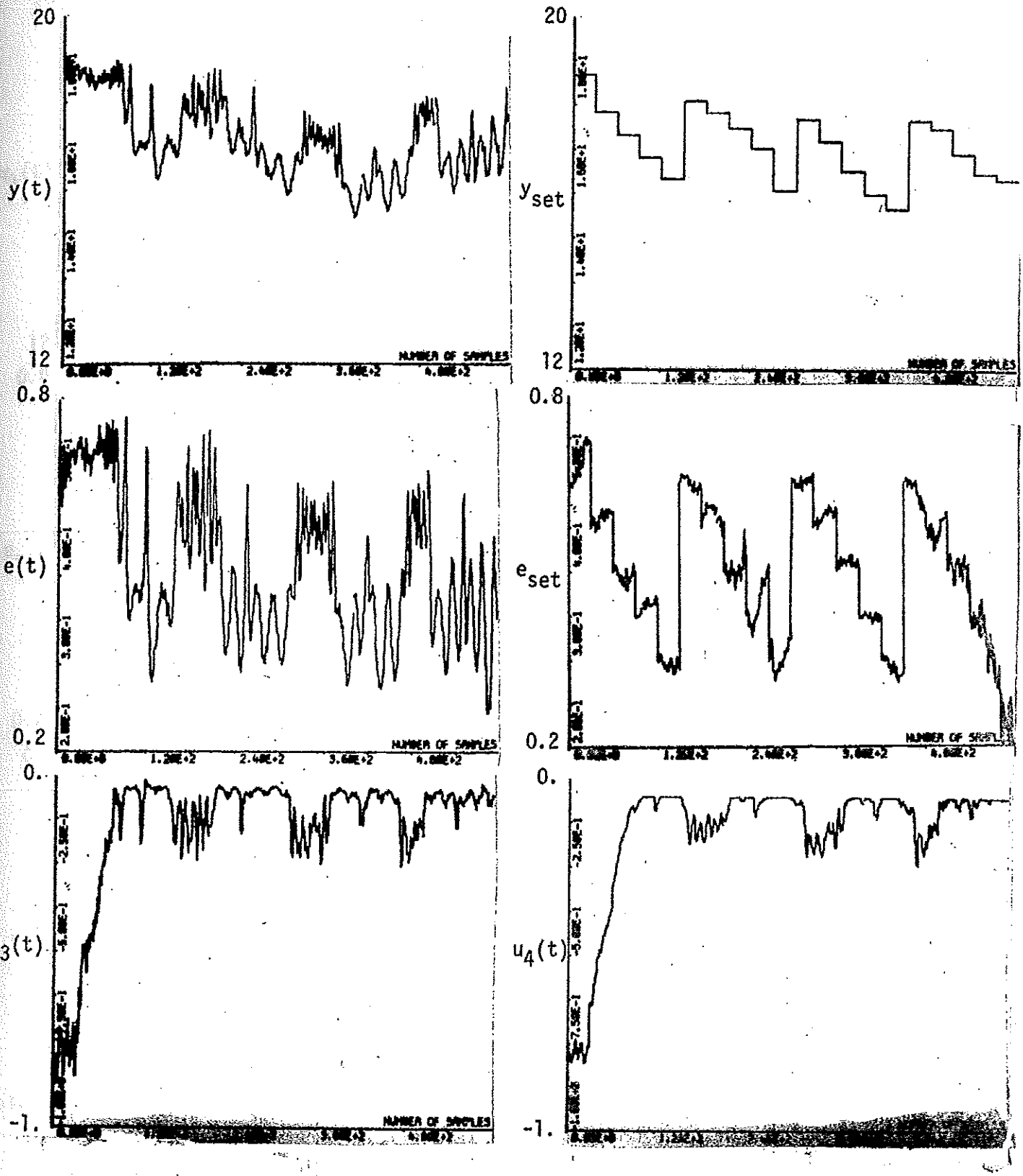

Figure 6.2 Experiment with the selftuning regulator.
$u_4(t) = - e_{set}/k$. The whole experiment length is
600 minutes

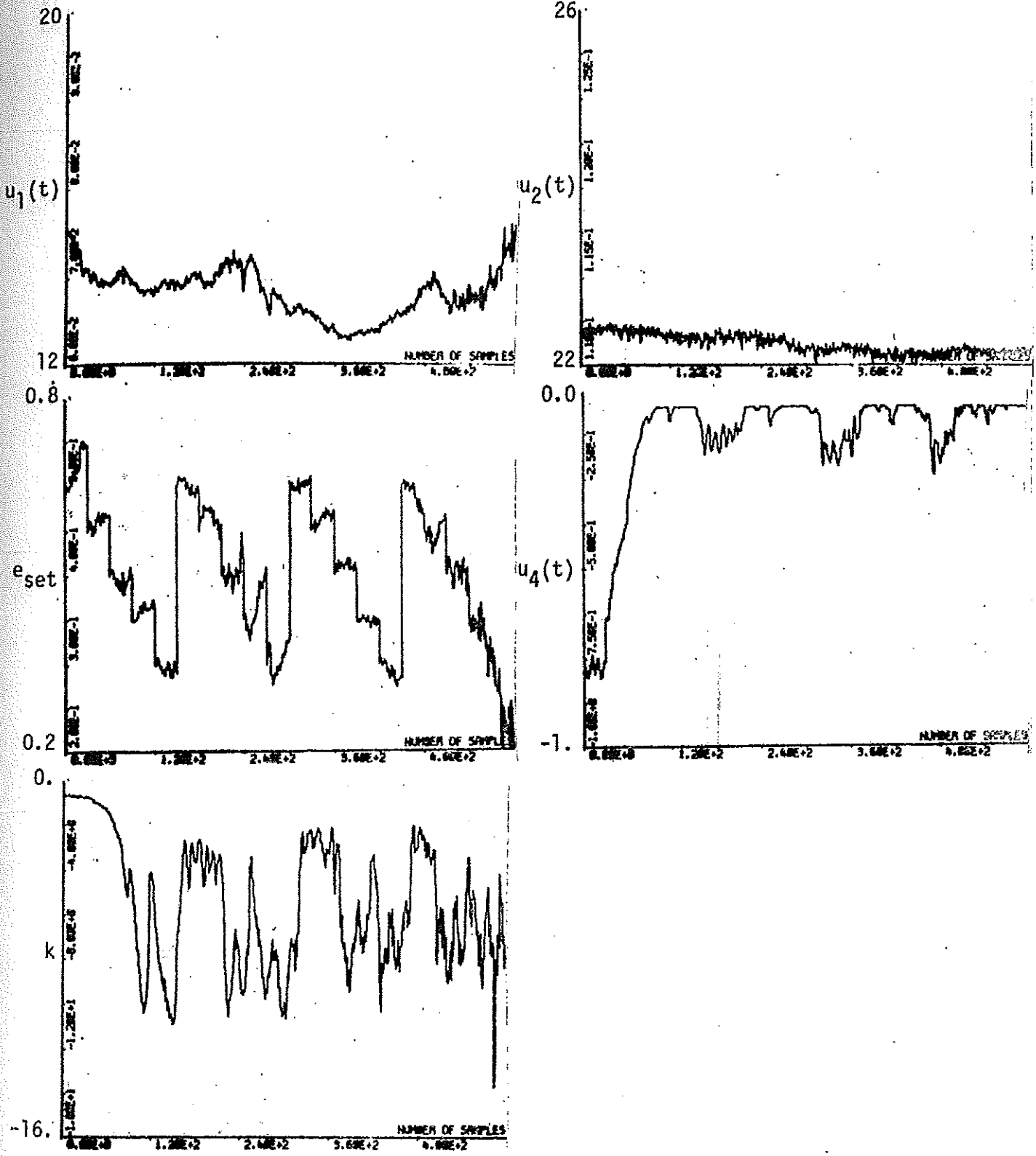

Figure 6.3 Experiment with the selftuning regulator. $u_4(t) = - e_{set}/k$. The whole experiment length is 600 minutes.

6.3 A selftuning regulator with two parameters

The regulator can be written as

$$u_4(t) = -(e_{set} - l)/k$$

where k and l are the parameters that are tuned. The regulator has been run in two different experiments.

The first experiment is simular to the experiment described in section 6.2. The temperature efficiency values have been the same and the forgetting factor has been 0.9, 0.8, 0.7 and 0.6. The result is shown in figure 6.4 and 6.5.

In the other experiment the exhaust air temperature has been raised about 1 ^{0}C by switching on the light for 35 minutes. All experiments have been made during nights. The controlled temperature has been the outdoor air temperature after the enthalpy exchanger (denoted implementation R2) and the air temperature after the inlet fan (denoted implementation R3) - see figure 4.2. Three efficiency levels have been used: 65%, 50% and 35%. Each level has been run for 100 minutes or 100 samples. The light was turned on after 30 minutes from the start at each level. The forgetting factor has been 0.9. The result is shown in figure 6.6 and 6.7.

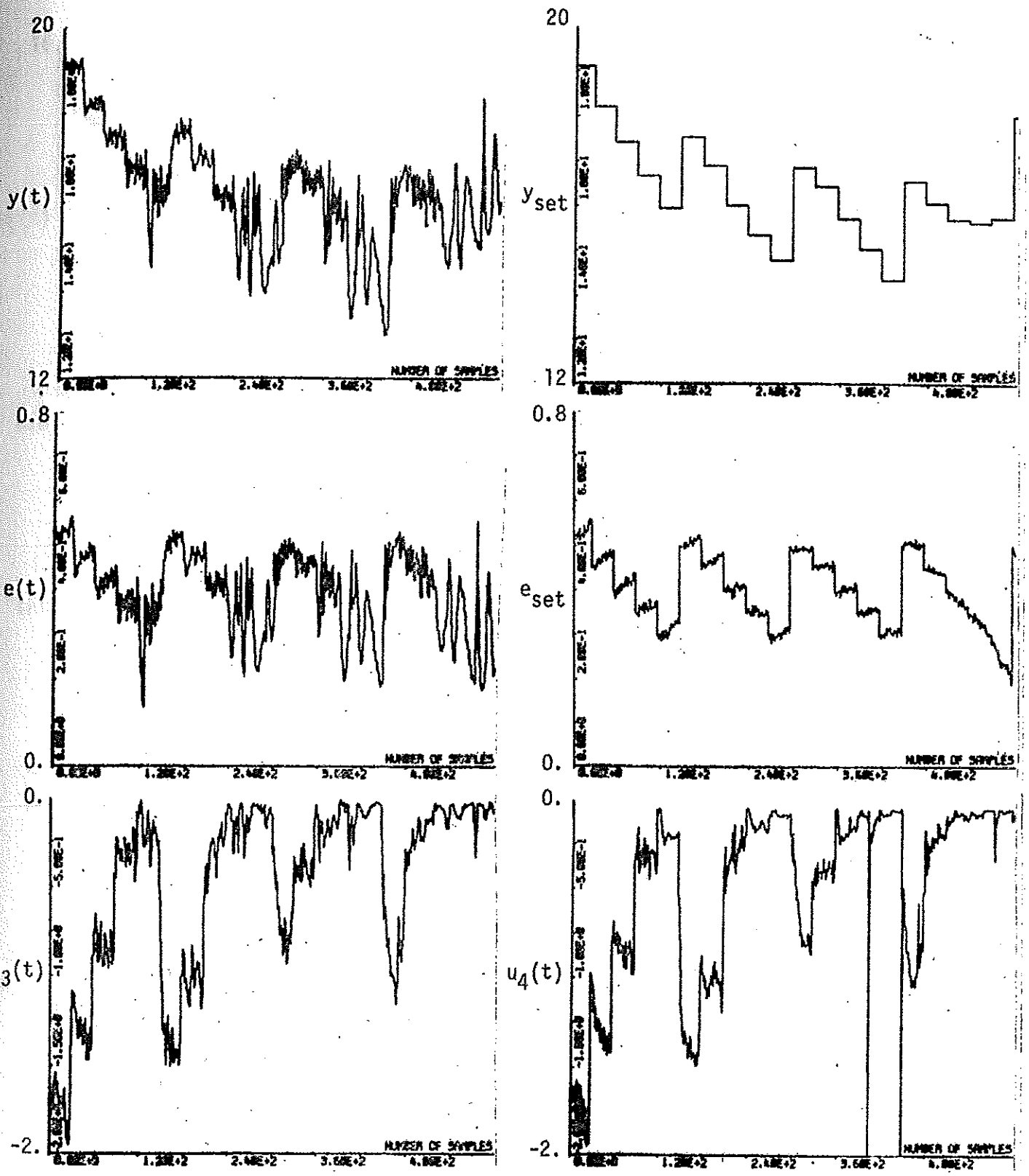

Figure 6.4 Experiment with the selftuning regulator.
$u_4(t) = -(e_{set} - 1)/k$. The whole experiment length is 600 minutes

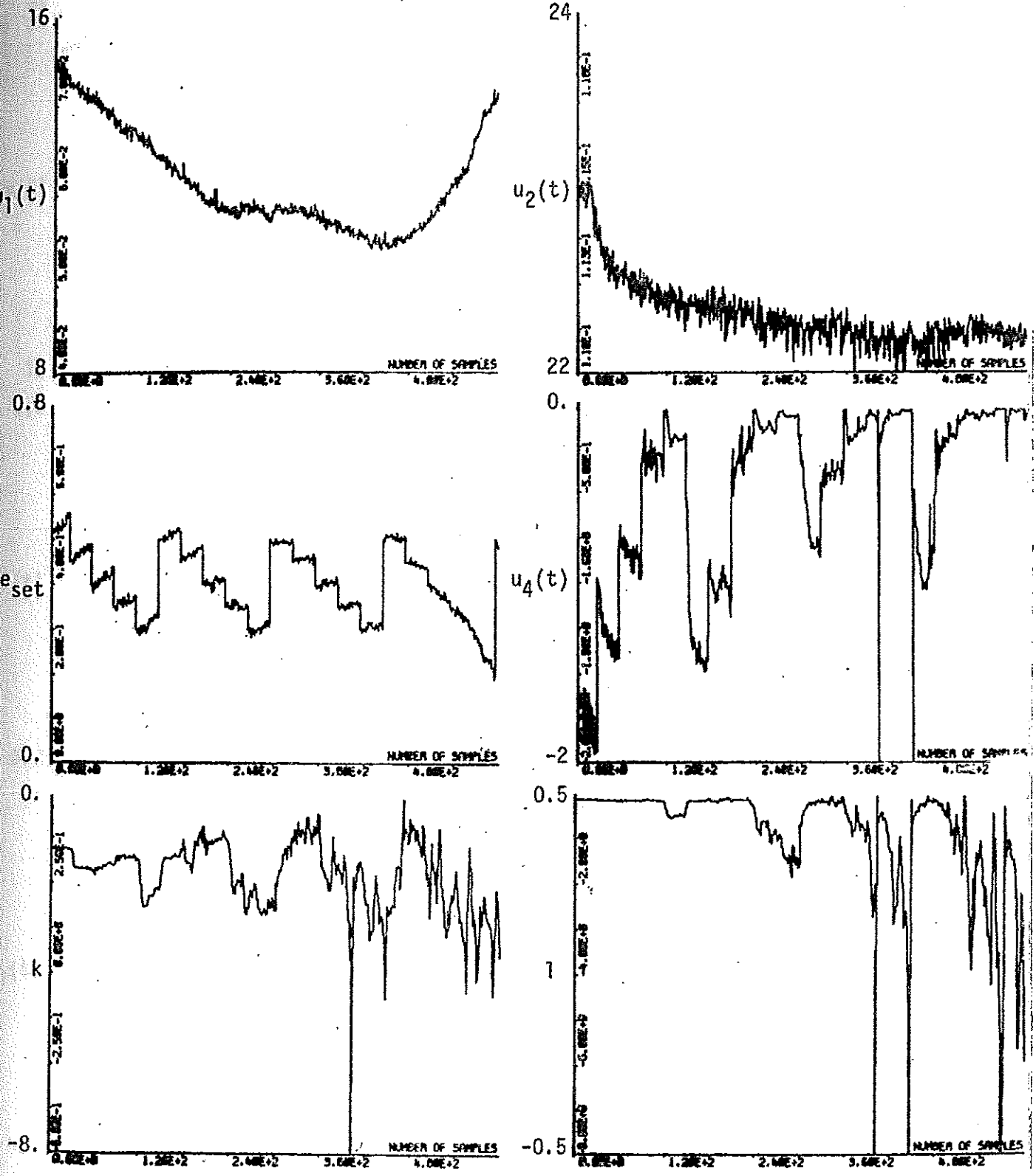

Figure 6.5 Experiment with the selftuning regulator
$u_4(t) = -(e_{set} - 1)/k$. The whole experiment length
is 600 minutes

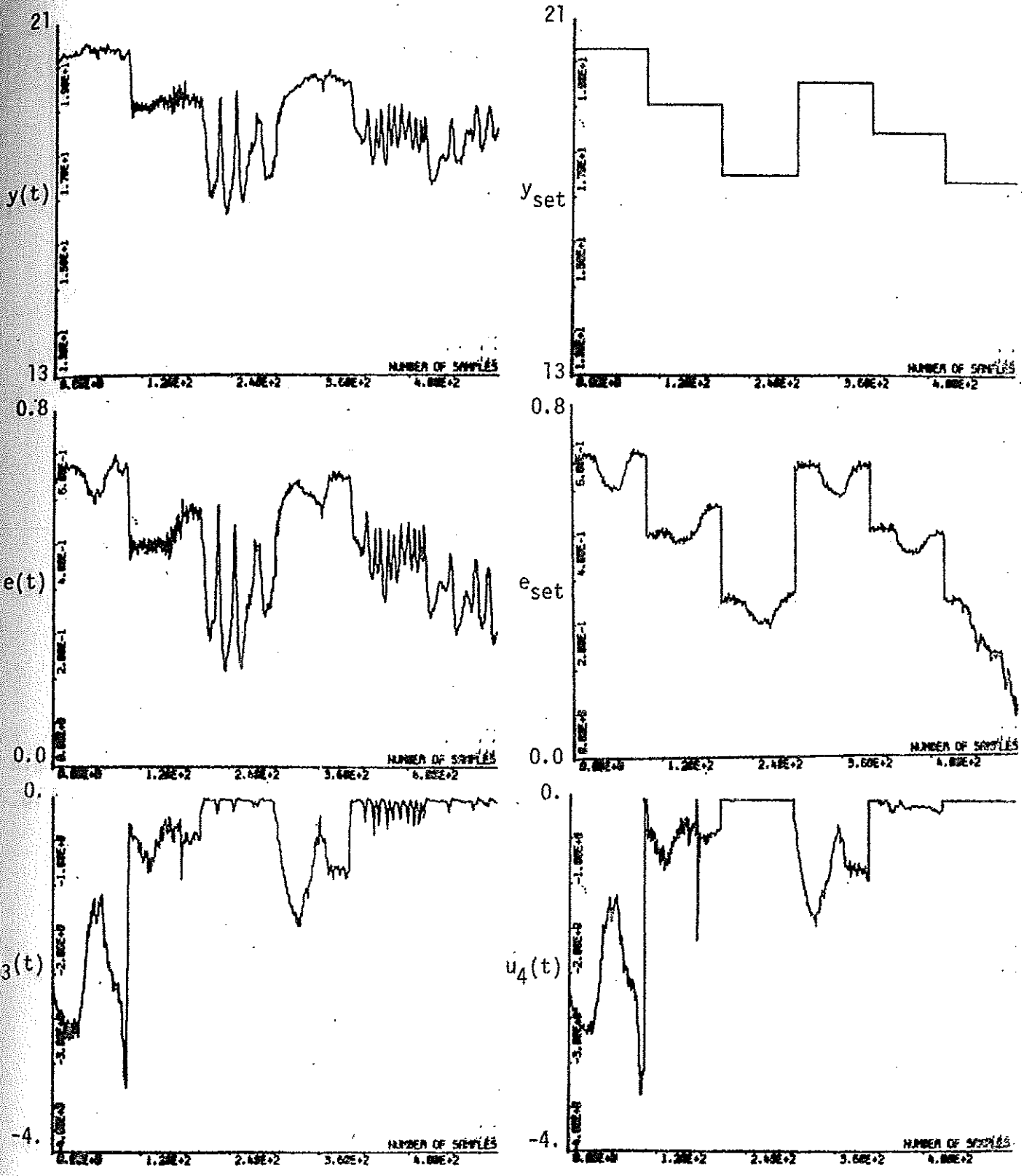

Figure 6.6 Experiment with the selftuning regulator $u_4(t) = -(e_{set} - 1)/k$. The whole experiment length is 600 minutes

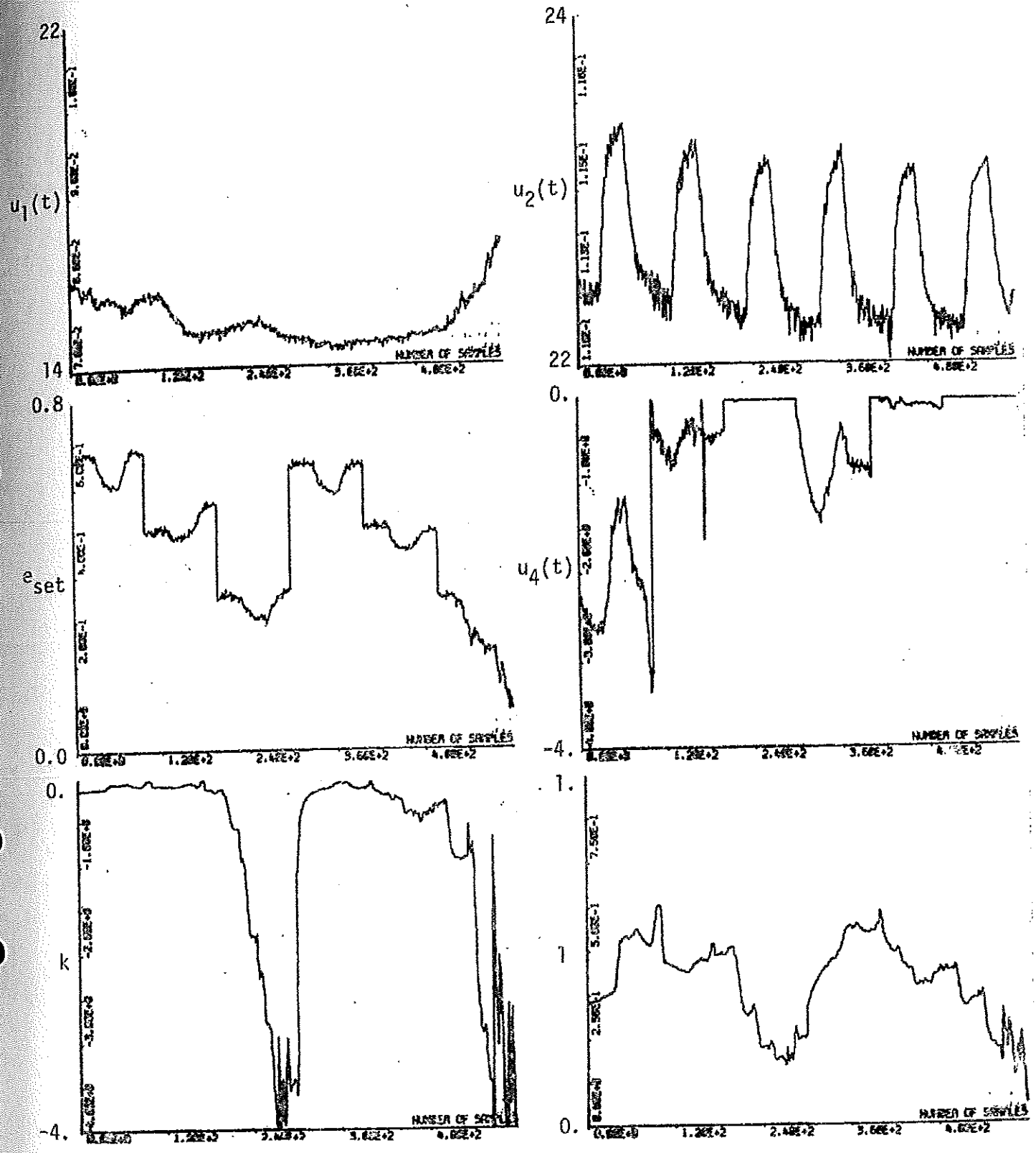

Figure 6.7 Experiment with the selftuning regulator $u_4(t) = -(e_{set} \quad 1)/k$. The whole experiment length is 600 minutes

7 Conclusions and remarks

The general conclusion about the fullscale control experiments is that high efficiency levels are easier to control than low ones. This is mainly due to the change of process gain, but also to uncontrollable revolution speed variations. This can be seen by comparing the measured revolution speed signal $u_3(t)$ and the revolution speed command signal $u_4(t)$.

The revolution speed has been less than 0.5 rpm when the uncontrollable revolution speed variations occured. It has been mentioned earlier that revolution speeds less than 0.5 rpm will be difficult to handle. The revolution speed has also been limited to the interval (0.05- 8.0) rpm. The revolution speed command signal $u_4(t)$ has been equal or close to the lower bound.

The experiments also show that the temperature efficiency can be about 30% at 0.05 rpm depending on the outdoor climate. This is a considerably high value in comparison with the models in section 3. This is the case when the outdoor air enthalpy is close to the exhaust air enthalpy. The enthalpy efficiency is close to zero, but the temperature efficiency and the moisture efficiency can still be large. This means that in this case the rotor must be stopped in order to prevent a too large temperature efficiency.

The temperature efficiency varies with the outdoor climate and how the enthalpy exchanger has been run earlier. This can be observed in the control experiments.

The selftuning regulator (implementation R1) with only one parameter tracks the setpoint curve rather badly. The tracking is rather slow at high temperature efficiency levels. The parameter k has then to change considerably in order to change the temperature efficiency a little. The forgetting factor λ

must be rather small in order to get a fast tracking.

The selftuning regulator with two parameters (implementation R2 and R3) tracks the setpoint curve rather well. The tracking is also rather good at the setpoint changes. The implementation R2, where the temperature is controlled immediately after the enthalpy exchanger seems to be the best. The conditions have not been the same for the two implementations. The implementation R2 has been started up at the desired temperature efficiency level 65% before the logging started.

A summing up of the conclusions are as follows

High temperature efficiency levels are easy to control.

Low temperature efficiency levels are difficult to control.

The temperature efficiency curve varies with the outdoor climate and how the enthalpy exchanger has been run earlier.

The temperature efficiency can be considerably high at low revolution speeds in comparison with models based on construction data.

The revolution speed has to be well controlled at low revolution speed in order to obtain good temperature efficiency control.

The selftuning regulator with two parameters (implementation R2) controls the process with fairly good result.

The rotor must be stopped in some cases depending on the climate in order to prevent a too large temperature efficiency.

8 References

Davis, W.D.T., 1970, System Identification for self-adaptive control. John Wiley and son.

Gustavsson, I., Selander, S. and Wieslander, J., 1973, IDPAC user's guide (Lund Institute of Technology, Division of Automatic Control) Report 7331. Lund

Jensen, L.H., (1973b), Ett coupler/controller system (Institutionerna för byggnadskonstruktionslära och reglerteknik Lunds Tekniska Högskola) Arbetsrapport 1973:6, Lund. (in Swedish)

Jensen, L.H., (1974), Computer programs for fullscale experiments (Department of Building Science and Division of Automatic Control, Lund Institute of Technology) Forthcoming report.

Wieslander, J., 1969, Real time identification - part I (Lund Institute of Technology, Division of Automatic Control) Report 6908, Lund.

Aström, K.J., 1968, Lectures on the Identification Problem - the Least Squares Method. (Lund Institute of Technology, Division of Automatic Control) Report 6806. Lund

Appendix 1

The static relation between the states and the inputs are

$$(k+1)x_1 = k \quad x_2 + u_1$$
$$(k+1)x_2 = k \quad x_1 + u_2$$

The cold side variables x_2 and u_1 can be computed from the hot side variables x_1 and u_2 as follows

$$x_2 = -1/(k+1)u_2 + k/(k+1)x_1$$
$$u_1 = -k/(k+1)u_2 + (2k+1)/(k+1)x_1$$

or on matrix form

$$\begin{bmatrix} x_2 \\ u_1 \end{bmatrix} = \begin{bmatrix} 1/(k+1) & k/(k+1) \\ -k/(k+1) & (2k+1)/(k+1) \end{bmatrix} \begin{bmatrix} u_2 \\ x_1 \end{bmatrix} = B \begin{bmatrix} u_2 \\ x_1 \end{bmatrix}$$

The efficiency x_1 for one compartment is computed by setting $u_1=0$ and $u_2=1$ which gives

$$x_1 = -b_{21}/b_{22}$$

If n compartment models are coupled in cascade then are the cold side variables given by the hot side variables as follows:

$$\begin{bmatrix} x_2^1 \\ u_1^1 \end{bmatrix} = B^n \begin{bmatrix} u_2^n \\ x_1^n \end{bmatrix} = C \begin{bmatrix} u_2^n \\ x_1^n \end{bmatrix}$$

and the efficiency x_1^n is computed as before

$$x_1^n = - c_{21}/c_{22}$$

Appendix 2

Eigenvalues of different compartment models.

Second order model

k = 0.1	RE	IM
	-1.200	0.000
	-1.000	0.000

k = 1.0	RE	IM
	-3.000	0.000
	-1.000	0.000

k = 10.	RE	IM
	-21.000	0.000
	-1.000	0.000

Fourth order model

k = 0.1	RE	IM
	-2.558	0.000
	-1.642	0.000
	-2.100	0.435
	-2.100	-0.435

k = 1.0	RE	IM
	-4.732	0.000
	-1.268	0.000
	-3.000	1.000
	-3.000	-1.000

k = 10.	RE	IM
	-22.955	0.000
	-1.046	0.000
	-20.944	0.000
	-3.056	0.000

Eight order model

k = 0.1	RE	IM
	-5.767	0.000
	-2.433	0.000
	-3.026	1.159
	-3.026	-1.159
	-5.174	1.159
	-5.174	-1.159
	-4.100	1.536
	-4.100	-1.536

k = 1.0	RE	IM
	-8.486	0.000
	-1.512	0.000
	-3.311	1.963
	-3.311	-1.963
	-6.689	1.963
	-6.689	-1.963
	-5.000	2.483
	-5.000	-2.483

k = 10.	RE	IM
	-27.091	0.000
	-0.909	0.000
	-24.811	0.000
	-3.189	0.000
	-20.567	0.000
	-7.433	0.000
	-22.284	0.000
	-5.716	0.000

Appendix 3

Determination of distance function d(k,l,y,x).

Definitions see figure A.1.

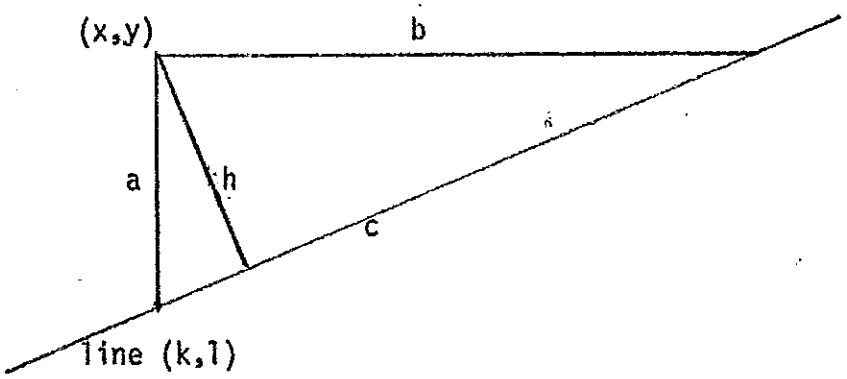

Fundamental geometri gives

$$d(k,l,y,x) = h$$

$$hc = ab$$

$$h = ab/c$$

$$a = y - kx - l$$

$$b = a/k$$

$$c^2 = a^2 + b^2$$

$$h^2 = a^4/(a^2 + a^2/k^2)k^2$$

$$h^2 = a^2/(k^2 + 1.)$$

$$d^2(k,l,y,x) = \frac{(y-kx-l)^2}{(k^2 + 1.)}$$